Comunidad de Madrid

GOBIERNO DE ESPAÑA
MINISTERIO DE CIENCIA, INNOVACIÓN Y UNIVERSIDADES

Ciemat
Centro de Investigaciones Energéticas, Medioambientales y Tecnológicas

Large Scale Structure and BAO

Anna Porredon (CIEMAT, Madrid)

Exploring New Frontiers in Cosmology
Galileo Galilei Institute
6 July 2026

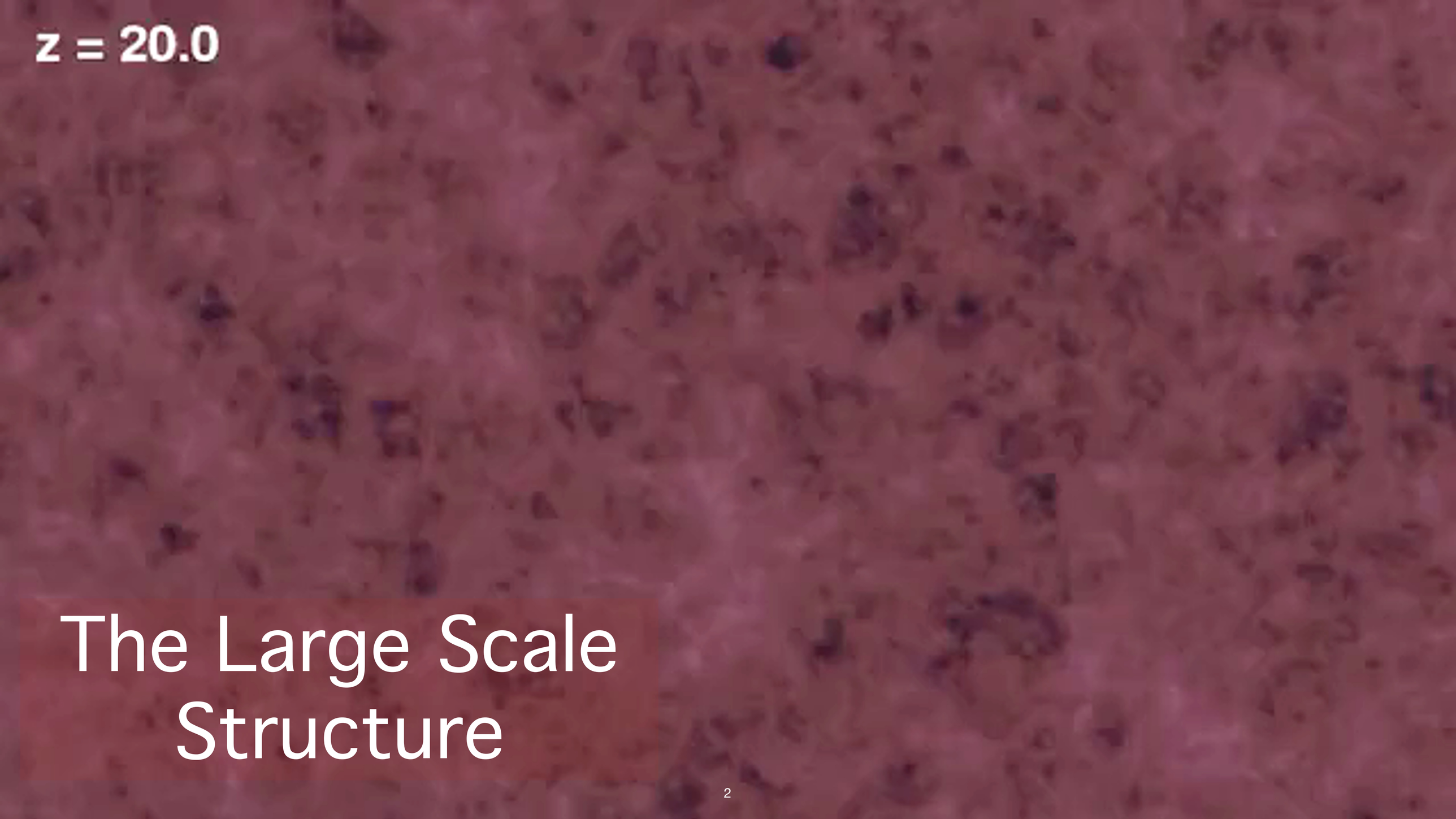

The Large Scale Structure

Evolution of the Universe

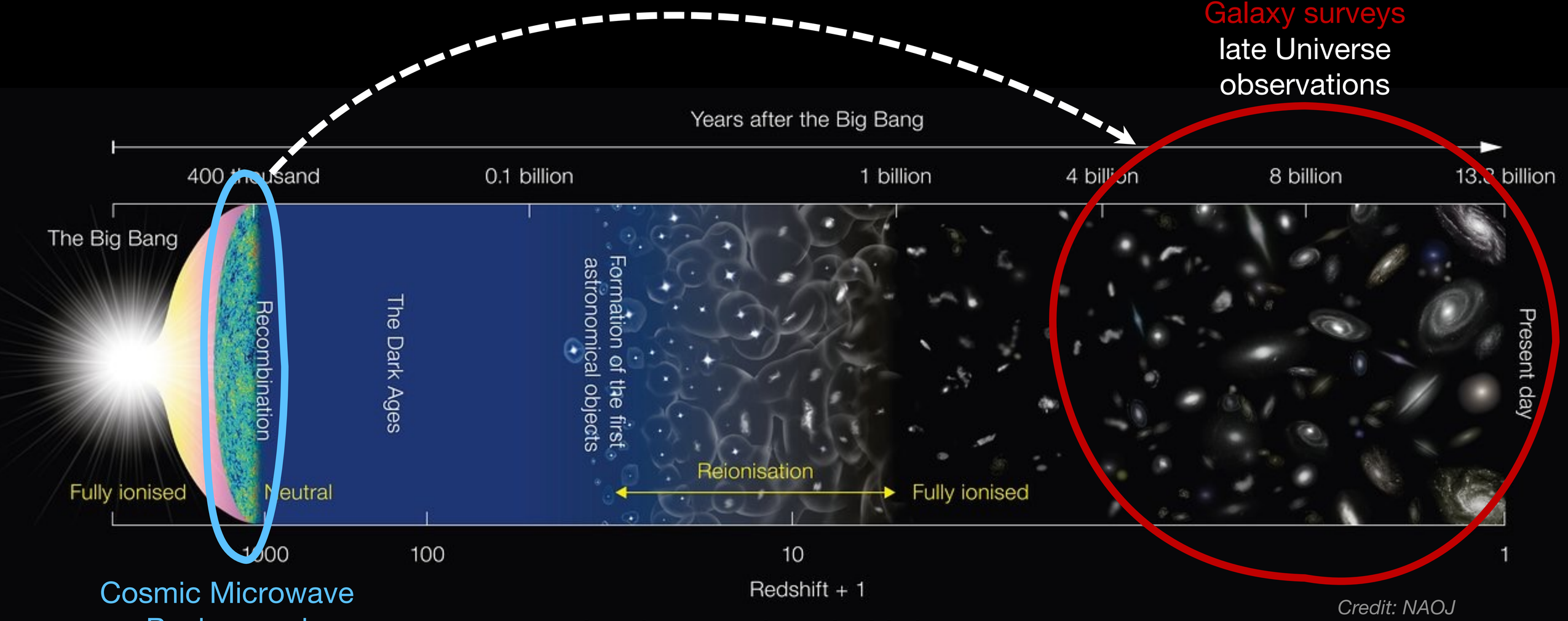

Galaxy surveys
late Universe
observations

Cosmic Microwave Background
early Universe
observations

Credit: NAOJ

Are late and early Universe observations compatible under ΛCDM?

Galaxy surveys

We can learn more about dark matter and dark energy by mapping the distribution of the large scale structure (tracer of the matter distribution in the Universe)

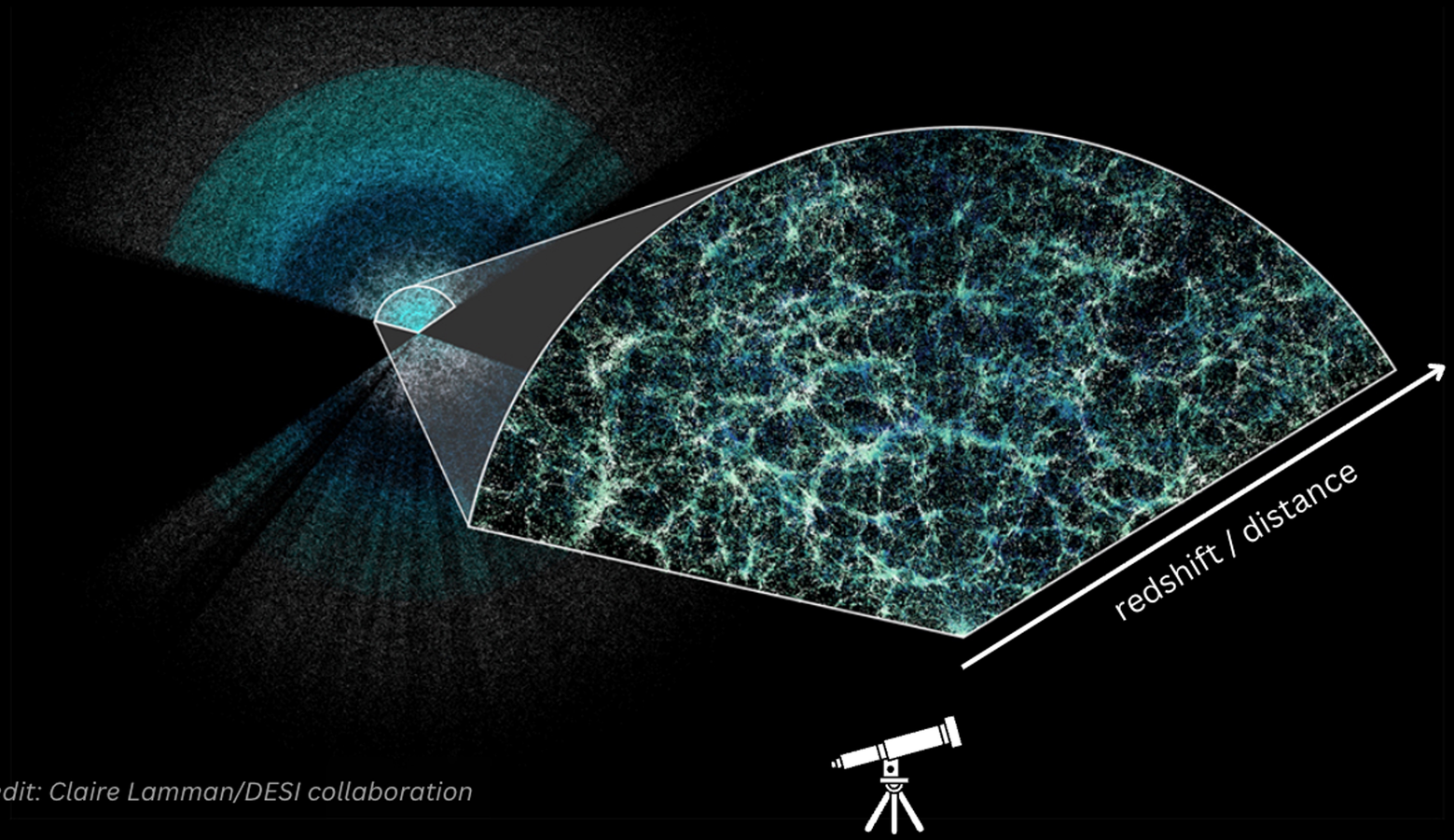

Credit: Claire Lamman/DESI collaboration

Galaxy clustering

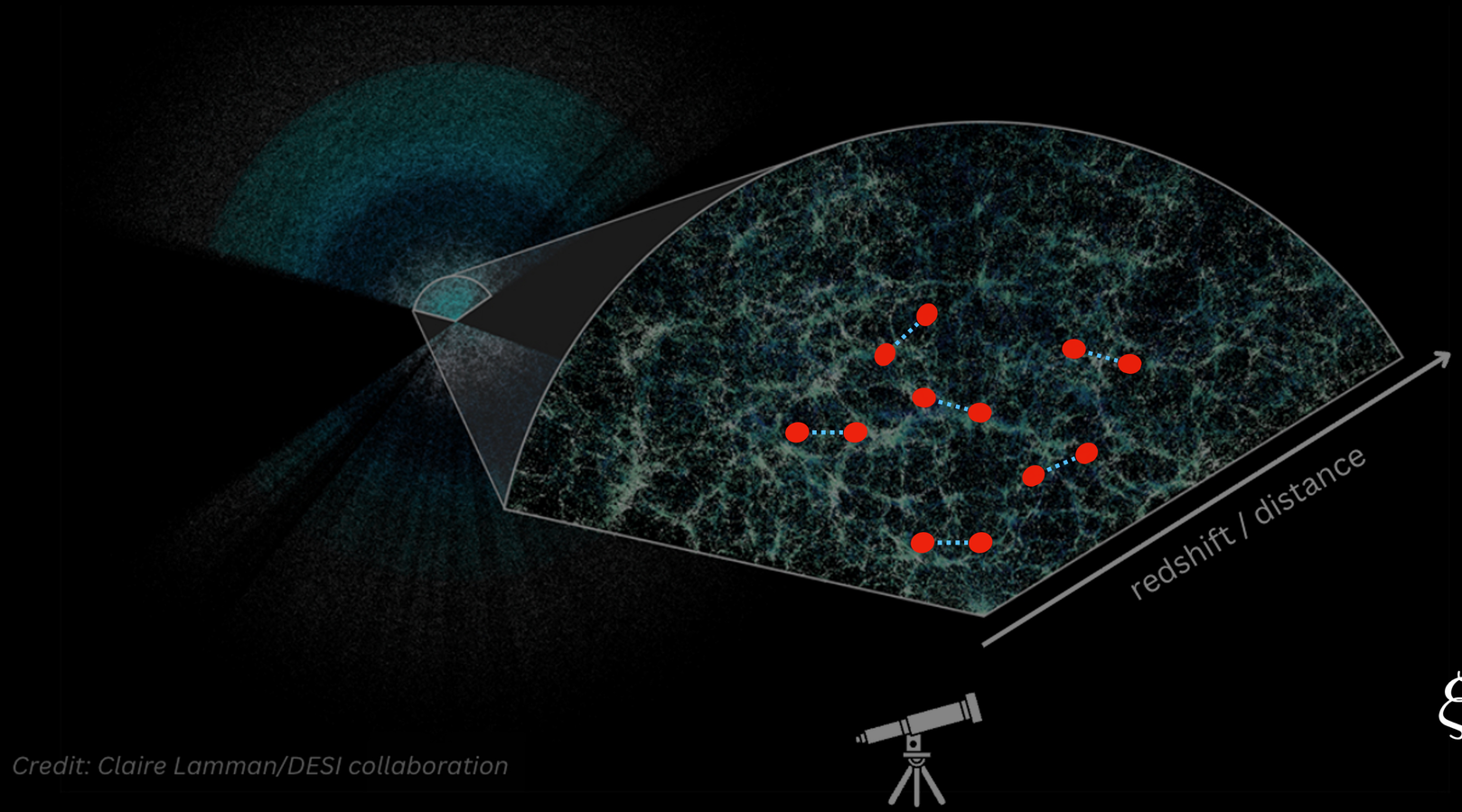

Credit: Claire Lamman/DESI collaboration

$$\delta(x) = \frac{\rho(x) - \bar{\rho}}{\bar{\rho}}$$

We can charaterise the density fluctuations with correlation functions, e.g. the 2-point correlation function:

$$\xi(R) = \langle \delta(x)\delta(x+R) \rangle$$

Due to statistical isotropy and homogeneity

Galaxy clustering 2PCF: physical interpretation

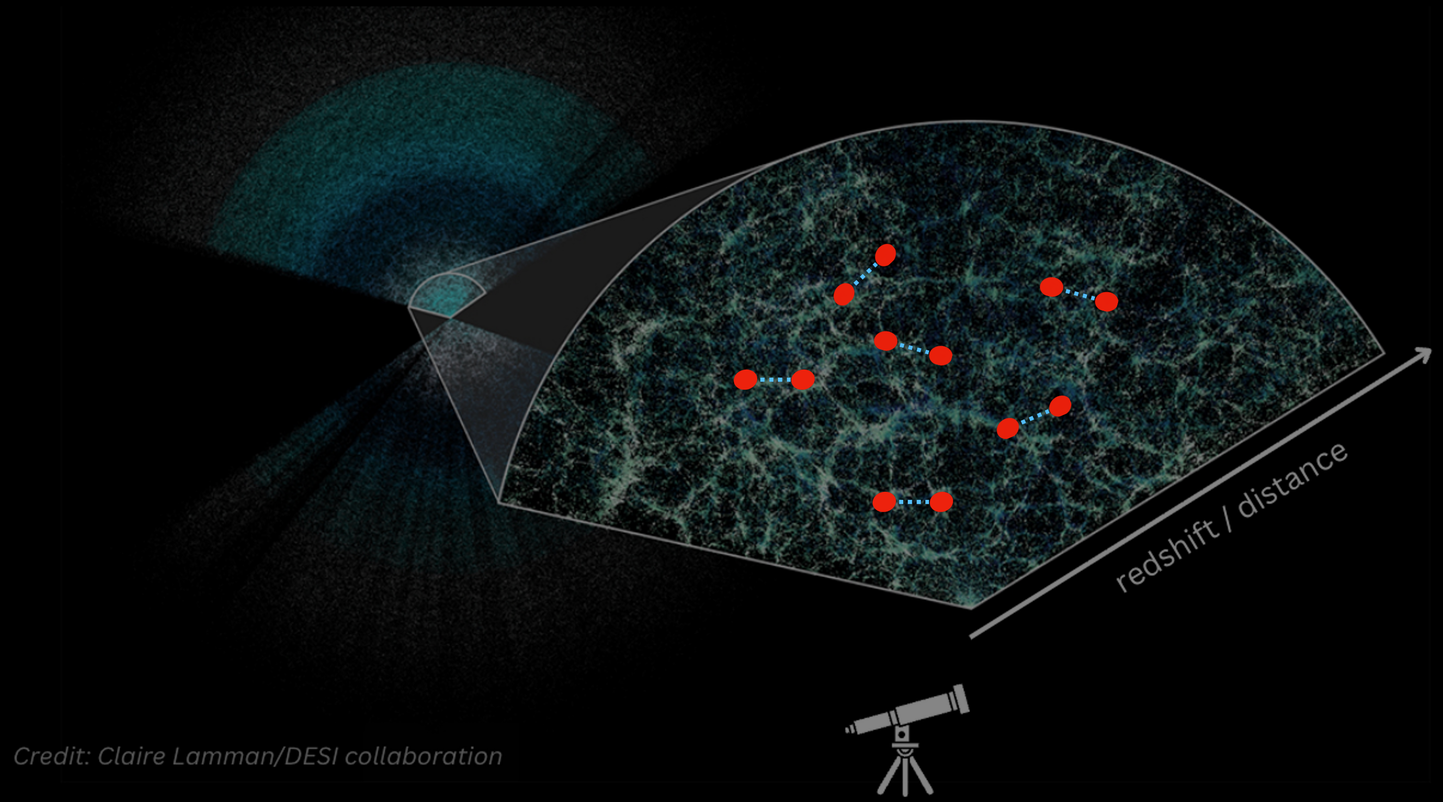

Credit: Claire Lamman/DESI collaboration

Excess over random probability (Poisson distribution) that two objects are separated by a distance *R*

$$dP = \rho_0^2[1 + \xi(R)]dV_1 dV_2$$

average density

Galaxy clustering 2PCF: measurement

To measure the 2PCF, we count pairs of galaxies separated by distance R and compare to the number of pairs from a random catalog under the same footprint

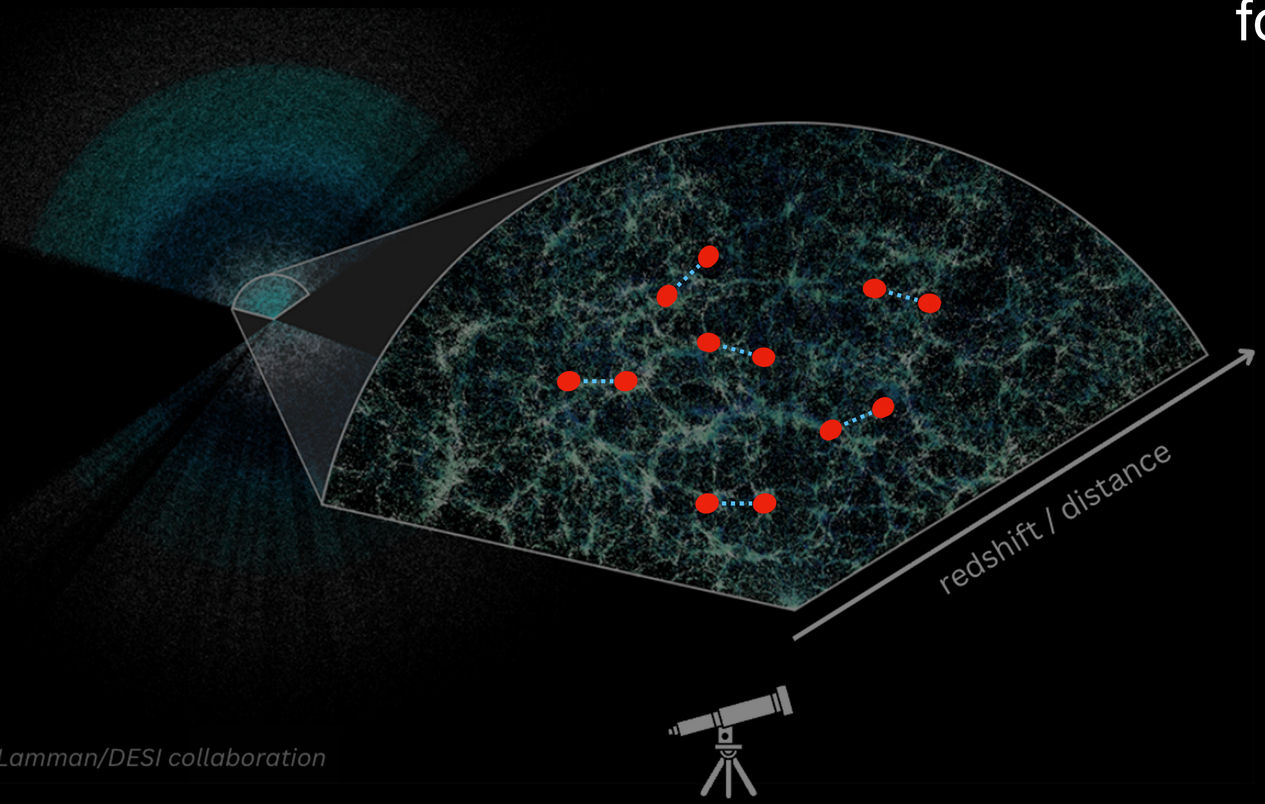

$$\xi(R) = \frac{DD - 2DR + RR}{RR}$$

Landy-Szalay Estimator

Galaxy clustering in Fourier

It is often convenient to work in Fourier space, with the power spectrum

$$\langle \delta(k)\delta(k')\rangle = (2\pi)^3 P(k)\delta_D^3(k-k').$$

$$P(k) = \int \mathrm{d}^3 r \xi(r) \mathrm{e}^{-ik\cdot r}$$

$$\xi(r) = \frac{1}{(2\pi)^3}\int \mathrm{d}^3 k P(k) \mathrm{e}^{ik\cdot r}$$

Galaxy clustering in Fourier

It is often convenient to work in Fourier space, with the power spectrum

$$\langle \delta(k)\delta(k') \rangle = (2\pi)^3 P(k) \delta_D^3(k - k').$$

$$P(k) = \int \mathrm{d}^3 r \xi(r) \mathrm{e}^{-ik\cdot r}$$

$$\xi(r) = \frac{1}{(2\pi)^3} \int \mathrm{d}^3 k P(k) \mathrm{e}^{ik\cdot r}$$

depending on the convention

Matter power spectrum

We typically characterize the amplitude of mass fluctuations with σ_8, defined as the expected variance of the overdensity δ in spheres of radius 8 Mpc/h

$$\sigma_8^2 = \langle \delta_8^2(x) \rangle \qquad \delta_8(x) = \int \mathrm{d}^3 x' \delta(x) W_R(x - x')$$

Matter power spectrum

We typically characterize the amplitude of mass fluctuations with σ_8, defined as the expected variance of the overdensity δ in spheres of radius 8 Mpc/h

$$\sigma_8^2 = \langle \delta_8^2(x) \rangle \qquad \delta_8(x) = \int \mathrm{d}^3 x' \delta(x) W_R(x - x')$$

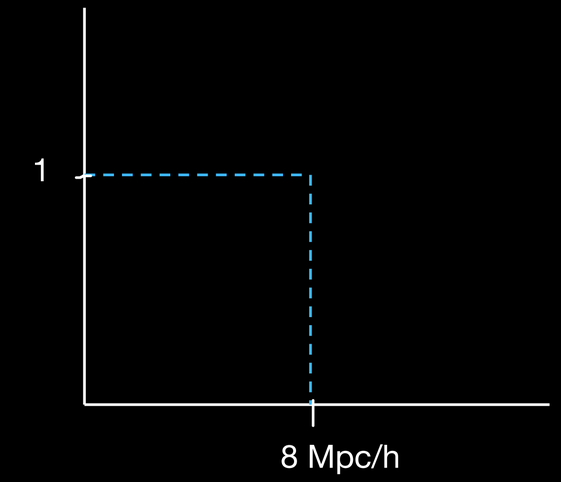

Matter power spectrum

We typically characterize the amplitude of mass fluctuations with σ_8, defined as the expected variance of the overdensity δ in spheres of radius 8 Mpc/h

~ size of massive galaxy clusters

$$\sigma_8^2 = \langle \delta_8^2(x) \rangle \qquad \delta_8(x) = \int \mathrm{d}^3 x' \delta(x) W_R(x - x')$$

$$\sigma_8^2(z=0) = \frac{1}{2\pi^2} \int \mathrm{d}k k^2 P(k, z=0) \tilde{W}_8^2(k)$$

$$\tilde{W}_8(k) = \frac{3 j_1(8k)}{8k}$$

What is the origin of these density fluctuations?

Evolution of inhomogeneities: inflation

Exponentially fast expansion of the very early Universe

$$a \propto \mathrm{e}^{Ht} \qquad H = \text{constant}$$

Origin of LSS: vacuum quantum fluctuations of the inflaton scalar field

Expected to be Gaussian, though current and future surveys aim to constrain primordial non-Gaussianities

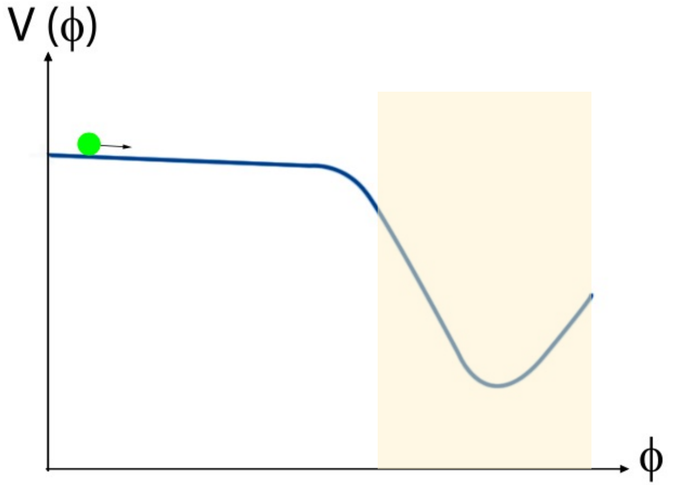

As the Universe expands, each wave generated by quantum fluctuations stretches out until its wavelength $\lambda = 1/H$, and then it freezes

Superposition of oscillating waves (stretching out) and frozen waves

Evolution of DM fluctuations

Inflation: $H^{-1} = \text{constant}$

Radiation: $H^{-1} \propto a^2$

Matter era: $H^{-1} \propto a^{3/2}$

$\lambda = 1/H$

$k = 2\pi/\lambda$

Evolution of fluctuations depends on whether they reenter the horizon in radiation domination (slower growth) or matter domination (faster growth)

Small-scale modes (higher k) enter the horizon earlier

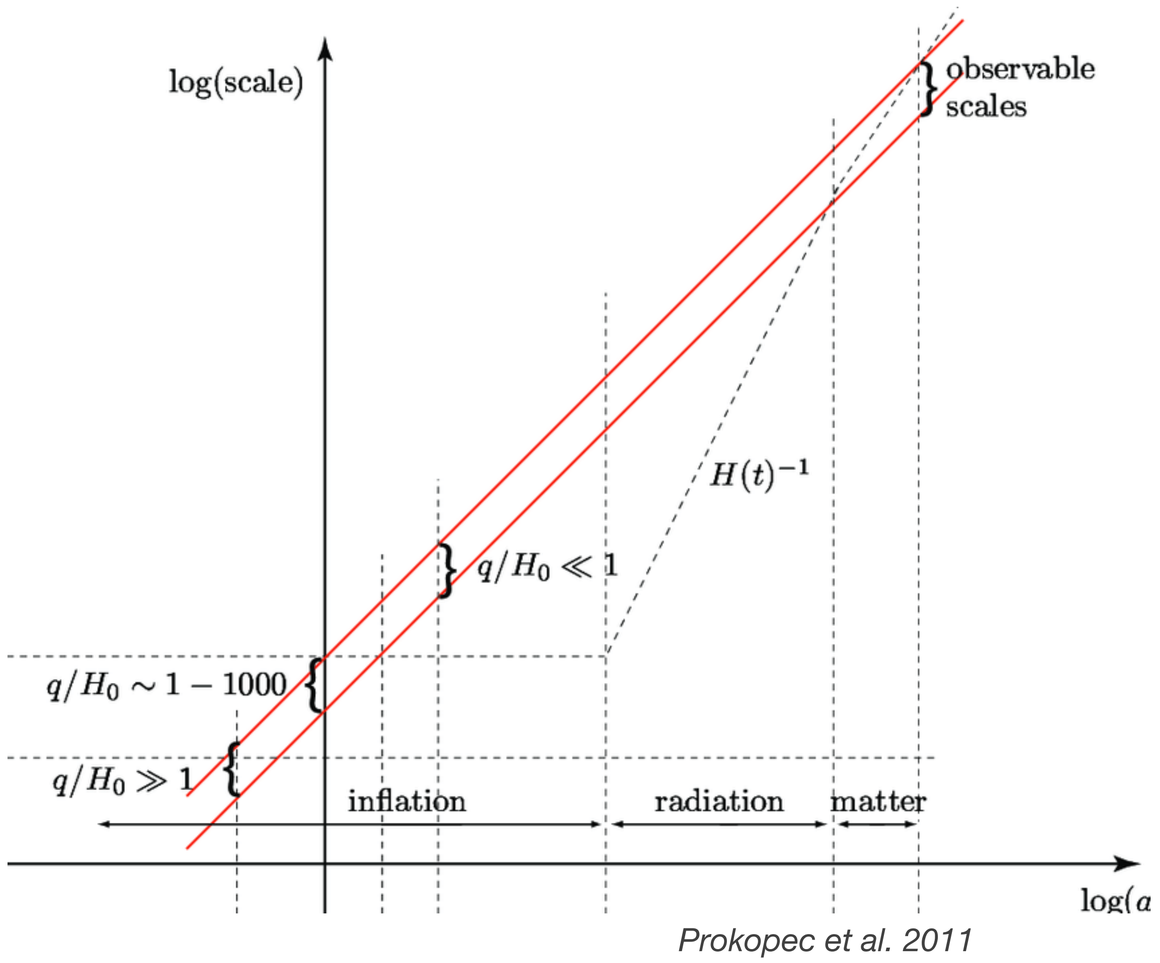

Prokopec et al. 2011

Evolution of DM fluctuations

At large scales (smaller k), modes reenter the horizon in the matter domination era, and we can use Newtonian physics, considering DM a non-relativistic fluid

$$\frac{\partial \mathbf{u}}{\partial t} + (\mathbf{u} \cdot \nabla_d)\,\mathbf{u} = -\frac{1}{\rho}\nabla_d P - \nabla_d \Phi$$

Euler equation
conservation of momentum

$$\frac{\partial \rho}{\partial t} + \nabla_d \cdot \rho \mathbf{u} = 0$$

Continuity equation
conservation of energy

$$\nabla^2 \Phi = 4\pi G \rho.$$

gravitational potential

Poisson equation

Evolution of DM fluctuations

1) Transforming from physical to comoving coordinates

$$\mathbf{d} = a(t)\mathbf{x}$$

$$\mathbf{u} = \dot{a}\mathbf{x} + a\dot{\mathbf{x}} = \dot{a}\mathbf{x} + \mathbf{v}$$

$$\mathrm{d}t = a\mathrm{d}\tau$$

$$\left(\frac{\partial}{\partial t}\right)_d = \frac{1}{a}\left(\frac{\partial}{\partial \tau}\right)_x - \frac{H}{a}(\mathbf{x}\cdot\nabla_x)$$

$$\nabla_d = \frac{1}{a}\nabla_x$$

Evolution of DM fluctuations

2) Considering perturbations of the density, velocity and gravitational potential

$$\rho = \bar{\rho}(1+\delta)$$

$$\mathbf{u} = H\mathbf{d} + \mathbf{v}$$

$$\Phi = \bar{\Phi} + \phi = \frac{2\pi G}{3}\bar{\rho}d^2 + \phi$$

Evolution of DM fluctuations

3) For matter, in the matter dominated era:

$$\bar{\rho_m} = \rho_{\rm crit}\Omega_m = \frac{3H^2}{8\pi G}\Omega_m$$

$$\bar{\rho}_m = \bar{\rho}_{m,0}a^{-3}$$

Evolution of DM fluctuations

Applying 1-3), we have:

$$\dot{\delta} + \nabla \cdot ((1+\delta)v) = 0$$ Continuity equation

$$\dot{v} + Hv + (v \cdot \nabla)v = -\frac{1}{\bar{\rho}(1+\delta)}\nabla P - \nabla\phi$$ Euler equation

$$\nabla^2\phi = \frac{3}{2}H^2\Omega_m\delta$$ Poisson equation

Evolution of DM fluctuations

The exact solution to these equations is nonlinear and cannot be solved completely analytically

At large scales, when $\delta \ll 1$, we can solve these at first order (linear regime)

$$\dot{\delta} + \nabla \cdot ((1+\delta)v) = 0$$ Continuity equation

$$\dot{v} + Hv + (v \cdot \nabla)v = -\frac{1}{\bar{\rho}(1+\delta)}\nabla P - \nabla\phi$$ Euler equation

$$\nabla^2\phi = \frac{3}{2}H^2\Omega_m\delta$$ Poisson equation

Evolution of DM fluctuations

Combining the three equations, and considering that $\mathrm{P} = 0$ for dark matter

Also convenient to move to Fourier scales, since the Fourier transform of $\nabla^2 \rightarrow -k^2$

$$\ddot{\delta}_k + 2H\dot{\delta}_k = 4\pi G\bar{\rho}\delta_k$$

Evolution of DM fluctuations

Combining the three equations, and considering that $\mathrm{P} = 0$ for dark matter

Also convenient to move to Fourier scales, since the Fourier transform of $\nabla^2 \rightarrow -k^2$

$$\ddot{\delta}_k + 2H\dot{\delta}_k = 4\pi G\bar{\rho}\delta_k$$

Damped harmonic oscillator

friction term:
resistance to the
growth of fluctuations

gravity enhances the growth of
fluctuations

Growth of linear perturbations: RD era

$$\ddot{\delta}_k + 2H\dot{\delta}_k = 4\pi G\bar{\rho}\delta_k$$

In the radiation domination era, the matter density is negligible, which simplifies the second order differential equation

$$a \propto t^{1/2}$$

$$4\pi G\bar{\rho}_m << H^2$$

Growth of linear perturbations: RD era

$$\ddot{\delta}_k + 2H\dot{\delta}_k = 4\pi\cancel{G}\bar{\rho}\delta_k$$

In the radiation domination era, the matter density is negligible, which simplifies the second order differential equation

$$a \propto t^{1/2}$$

$$4\pi G\bar{\rho}_m << H^2$$

$$\longrightarrow \quad \delta(t) = A_1 + A_2 \ln t$$

Extremely slow growth of density perturbations

Growth of linear perturbations: MD era

$$\ddot{\delta}_k + 2H\dot{\delta}_k = 4\pi G\bar{\rho}\delta_k$$

There are two solutions to this second-order differential equation: a growing and a decaying solution (which becomes negligible with time)

$$a \propto t^{2/3} \longrightarrow \delta(t) = A_1 t^{2/3} + A_2 t^{-1} \simeq a(t)$$

$$4\pi G\bar{\rho} = \frac{3}{2}H^2$$

Growth of linear perturbations: ΛD era

$$\ddot{\delta}_k + 2H\dot{\delta}_k = 4\pi\cancel{G}\bar{\rho}\delta_k$$

In the era dominated by Λ, the matter density becomes negligible again relative to vacuum energy

$$a \propto \exp(Ht) \longrightarrow \delta(t) = A_1 + A_2 \exp(-2Ht) \simeq \text{constant}$$

$$H(t) = H_\Lambda = \text{constant}$$

density perturbations stop growing

Growth of linear perturbations: *more general solution*

$$\ddot{\delta}_k + 2H\dot{\delta}_k = 4\pi G\bar{\rho}\delta_k$$

$$D(a) \equiv \delta(a)/\delta(a=1) \longrightarrow \ddot{D} + 2H\dot{D} = 4\pi G\bar{\rho}_m D$$

linear growth factor definition

The exact growing solution for ΛCDM is then:

$$D(a) = \frac{5\Omega_m}{2} H(a) \int_0^a \frac{\mathrm{d}a'}{(a'H(a'))^3}$$

Growth of linear perturbations: super-horizon modes

Until now we have seen the growth of linear perturbations after reentering the horizon (sub-horizon modes)

For super-horizon modes, we can obtain the growth of δ from the Poisson equation and enforcing that the gravitational potential is constant at super-horizon scales

$$\frac{1}{a^2}\nabla^2\Phi = 4\pi G\bar{\rho}\delta = 0 \longrightarrow -k^2\Phi = 4\pi G a^2\bar{\rho}\delta_k = 0$$

from changing to comoving coordinates

Radiation domination $\rho \propto a^{-4} \longrightarrow \delta \propto a^2$

Matter domination $\rho \propto a^{-3} \longrightarrow \delta \propto a$

Linear and nonlinear P(k)

Modes reentered the horizon recently, so we have the primordial power spectrum

(Peebles-Harrison-Zeldovich spectrum)

$$P_0(k) = A_s k^{n_s}$$

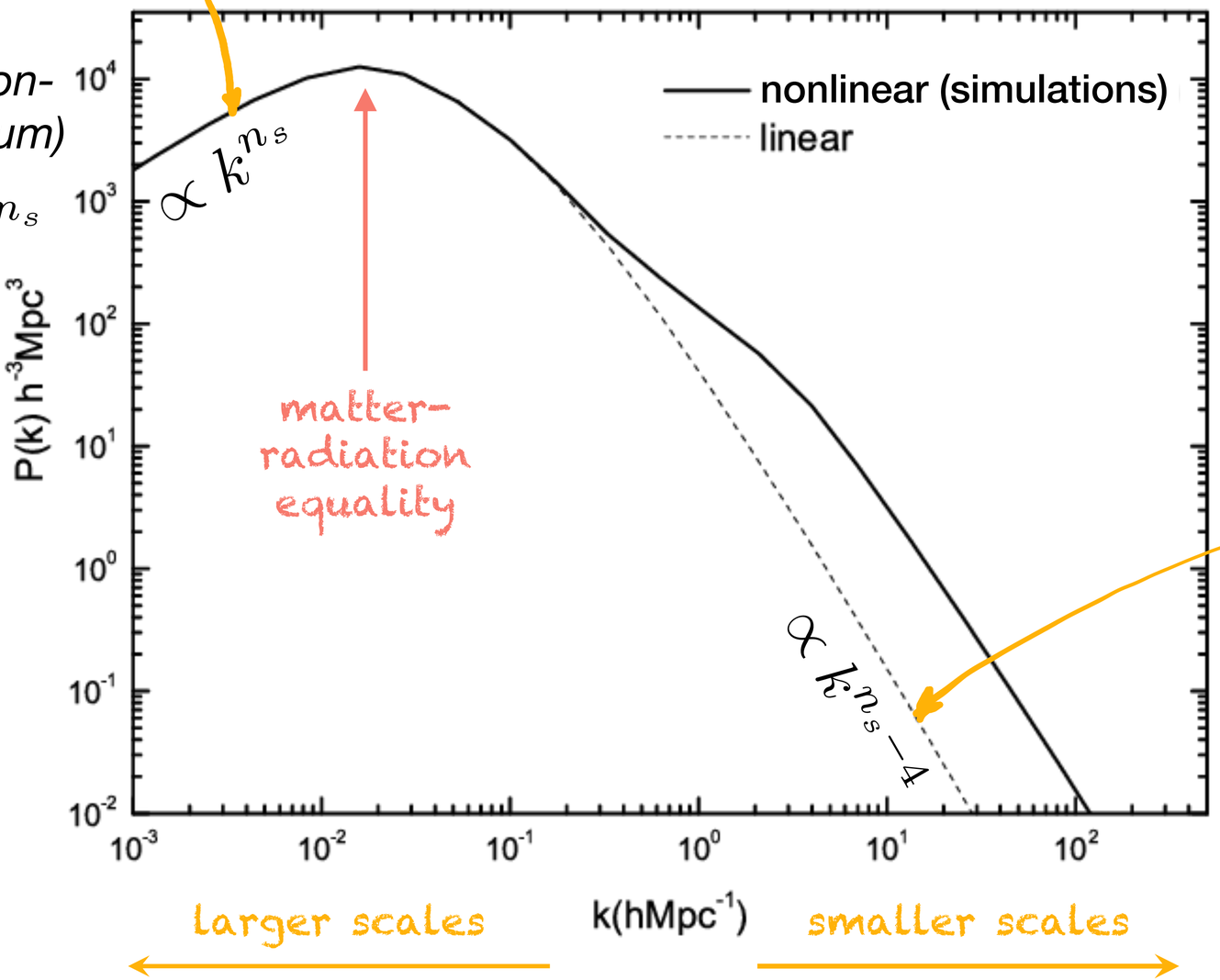

$$P_{\rm lin}(k,z) = D^2(z) P_{\rm lin}(k, z=0)$$

Modes reentered during radiation dominated era: *growth suppression*

Transfer function

The transfer function accounts for the suppression of growth during radiation domination ($\mathrm{T(k)} = 1$ for modes that enter during matter domination)

$$P(k) = A_s k^{n_s} T^2(k)$$

$$H \propto a^{-2}$$

A mode enters the horizon when $k = 2\pi/\lambda = 2\pi \mathrm{a} H \rightarrow k \propto a^{-1}$

Super-horizon growth $\delta \propto a^2$

Sub-horizon growth $\delta(t) = A_1 + A_2 \ln(t) \sim \ln(a)$

$$a \propto t^{1/2}$$

$$T(k) = \left(\frac{a_{entry}}{a_{eq}}\right)^2 \ln\left(\frac{a_{eq}}{a_{entry}}\right)$$

$$T(k) \propto k^{-2}$$

Regimes of structure formation

$$\delta(x) = \frac{\rho(x) - \bar{\rho}}{\bar{\rho}}$$

Linear regime

$\delta \ll 1$

Homogeneous growth, earlier times, large scales

Analytical calculations are possible

Transition to non-linear growth

$\delta \sim 1$

Can be computed with perturbation theory (but difficult)

Nonlinear structure formation couples k modes (not independent anymore)

Non-linear growth, late times

$\delta > 1$

Higher order perturbation theory (even more difficult)

Ultimately: direct simulation with N-body codes

Beyond 2pt

The power spectrum and 2PCF are the two-point moments of the field, and completely describe the statistical properties of a Gaussian random field.

However, given the nonlinear evolution of the growth of structure, there are higher order moments in the field not captured by the 2-pt statistics.

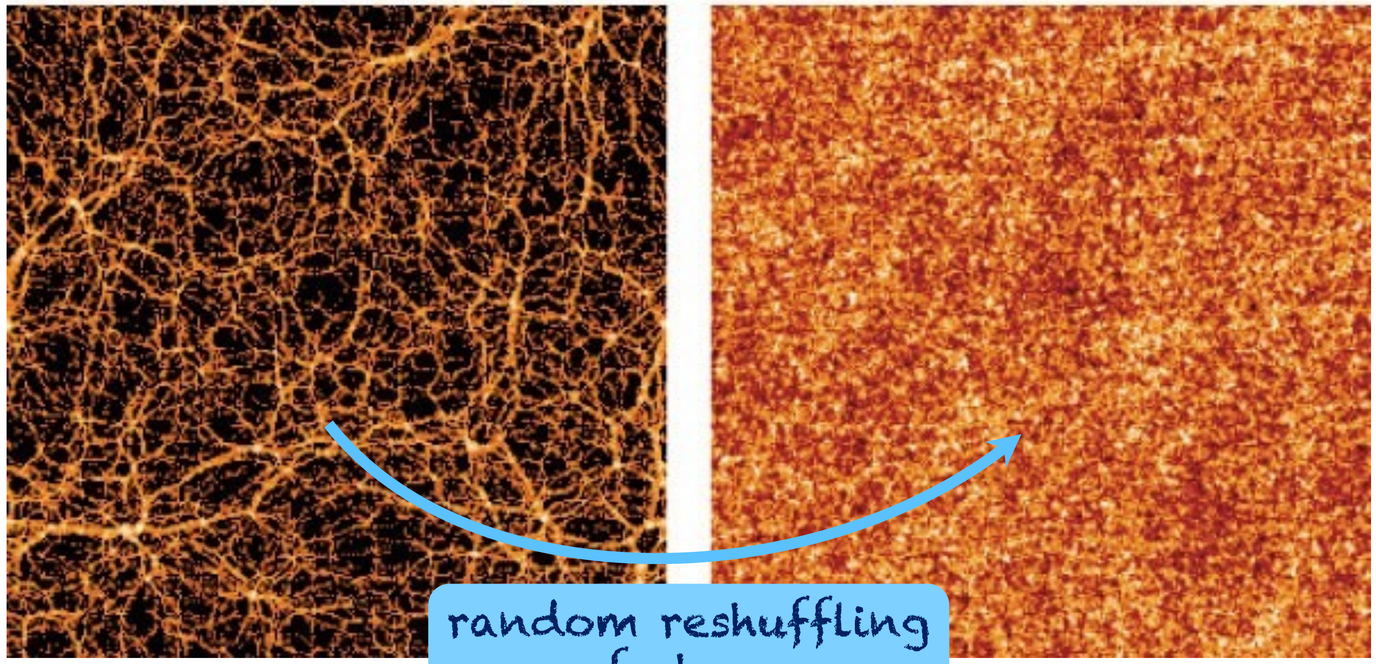

Peter Coles & Lung-Yih Chiang 2000

Same power spectrum, but completely different morphology!

Beyond 2pt

- Higher-order moments: bispectrum (3pt), trispectrum (4pt), …
- Other statistics to capture the non-gaussinity of the field: e.g. peak counts, minima counts, wavelet scattering transform, probability density function, …
- Field-level inference or simulation-based inference

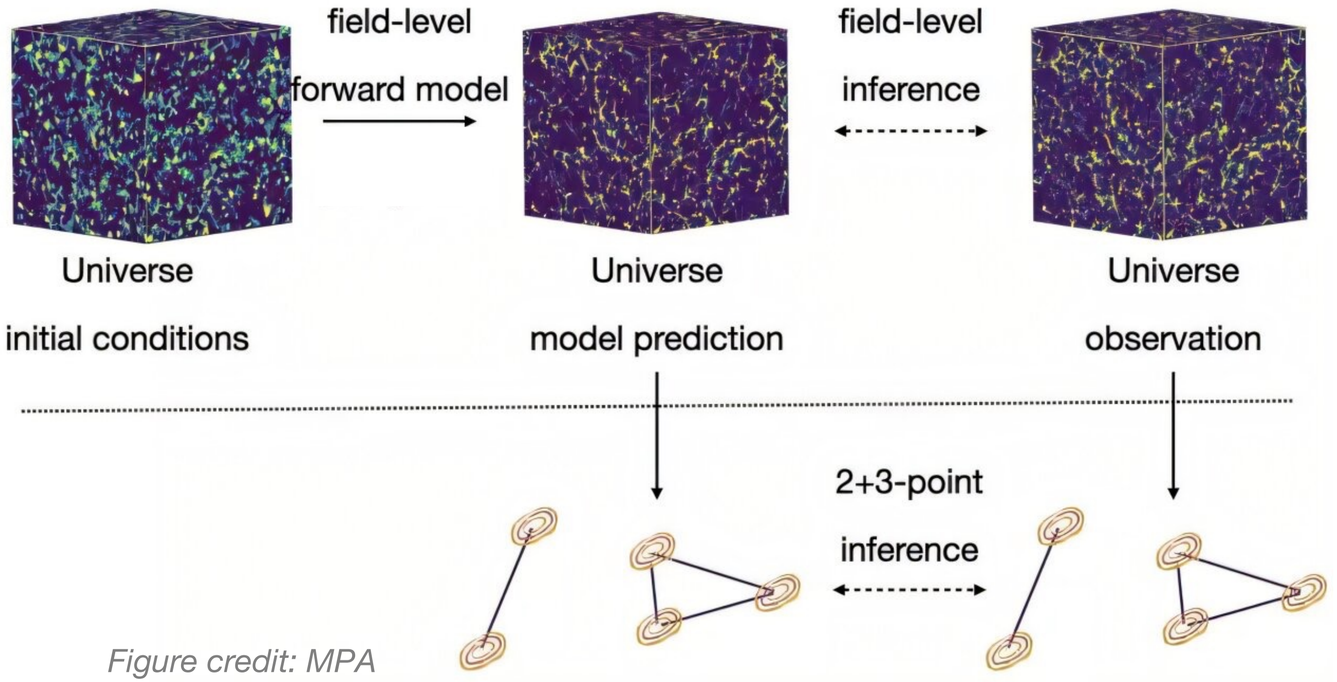

Figure credit: MPA

Galaxy bias

$$\delta_g = b\delta_m$$

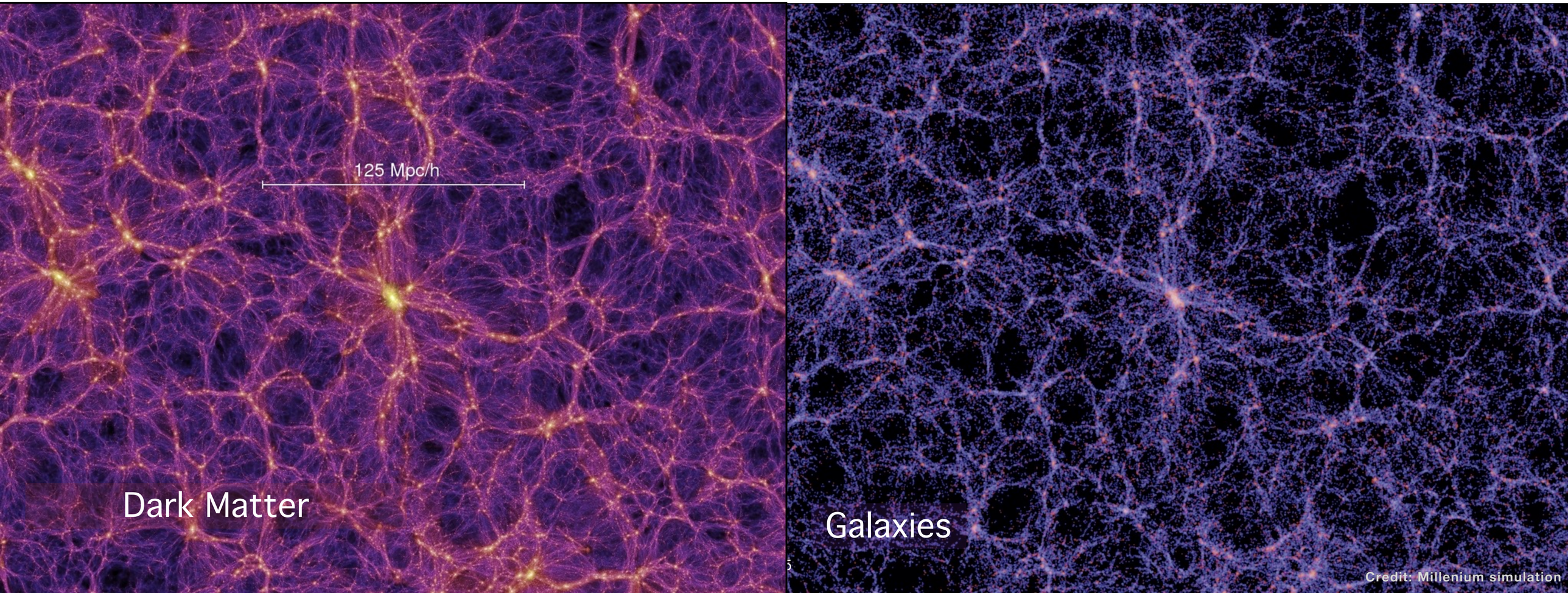

Baryon Acoustic Oscillations

The interplay between gravity and pressure in the early-Universe hot plasma generated sound waves that propagated through it

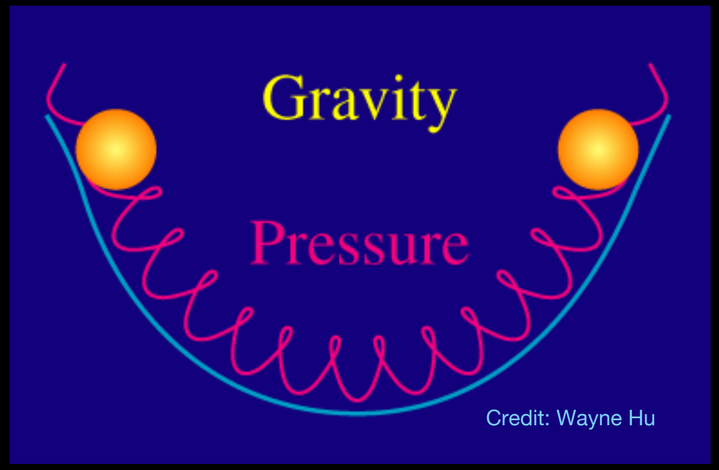

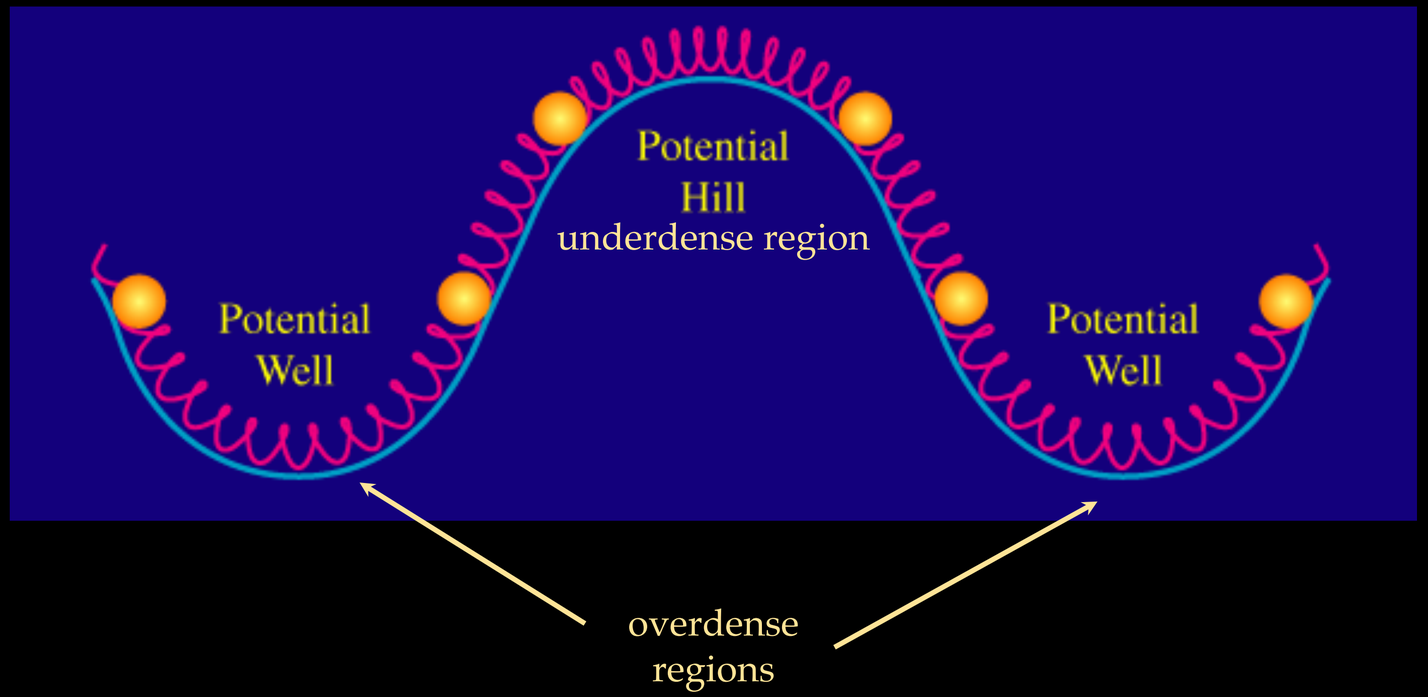

Baryon Acoustic Oscillations

At the time of decoupling, the waves froze, leaving an imprint on the CMB (last scattering surface) and the distribution of matter

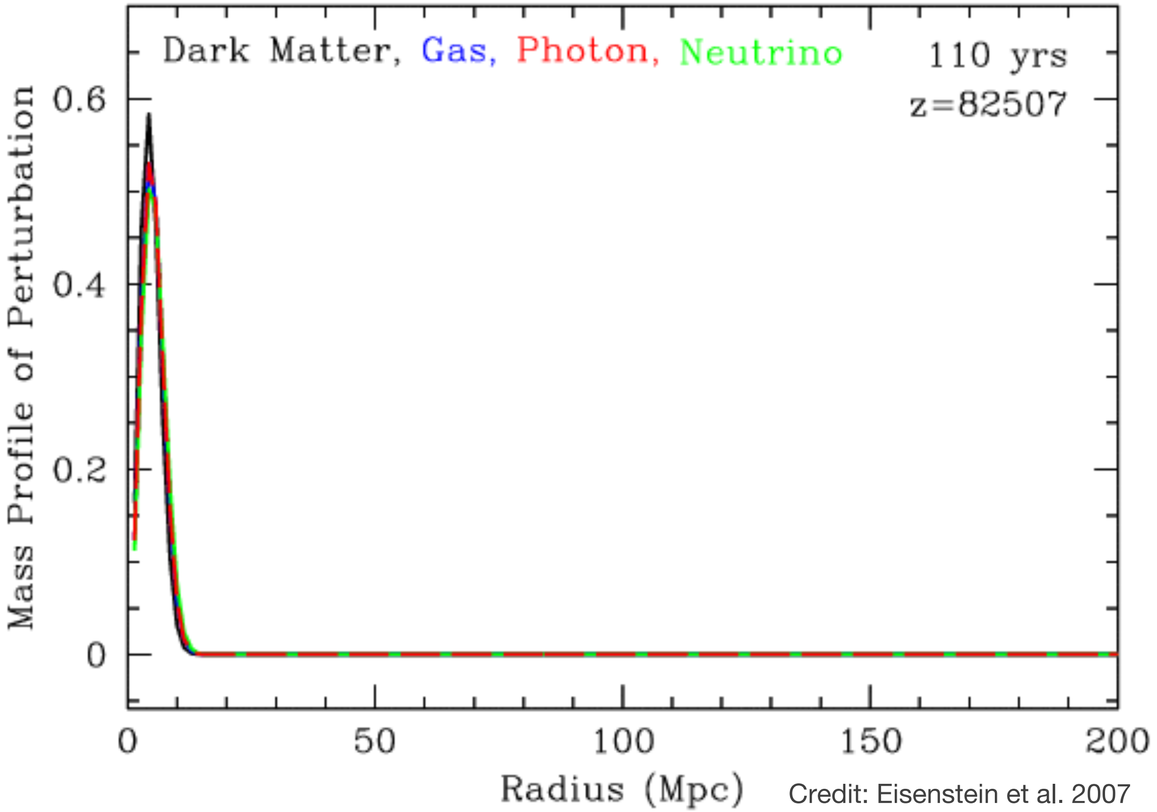

Credit: Eisenstein et al. 2007

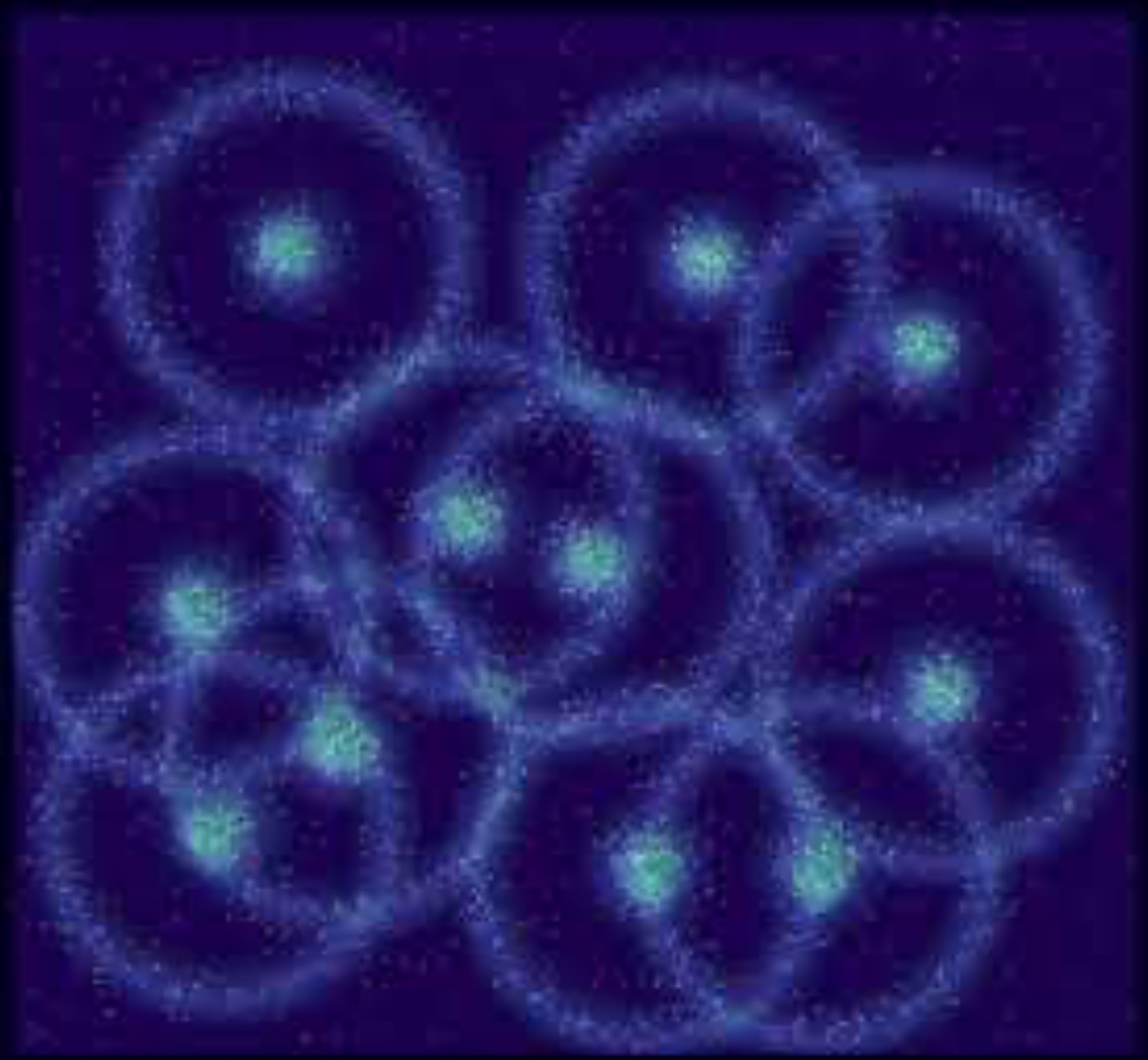

Baryon Acoustic Oscillations

This particular scale (~150 Mpc) can still be observed today in the distribution of galaxies and serves as a standard ruler

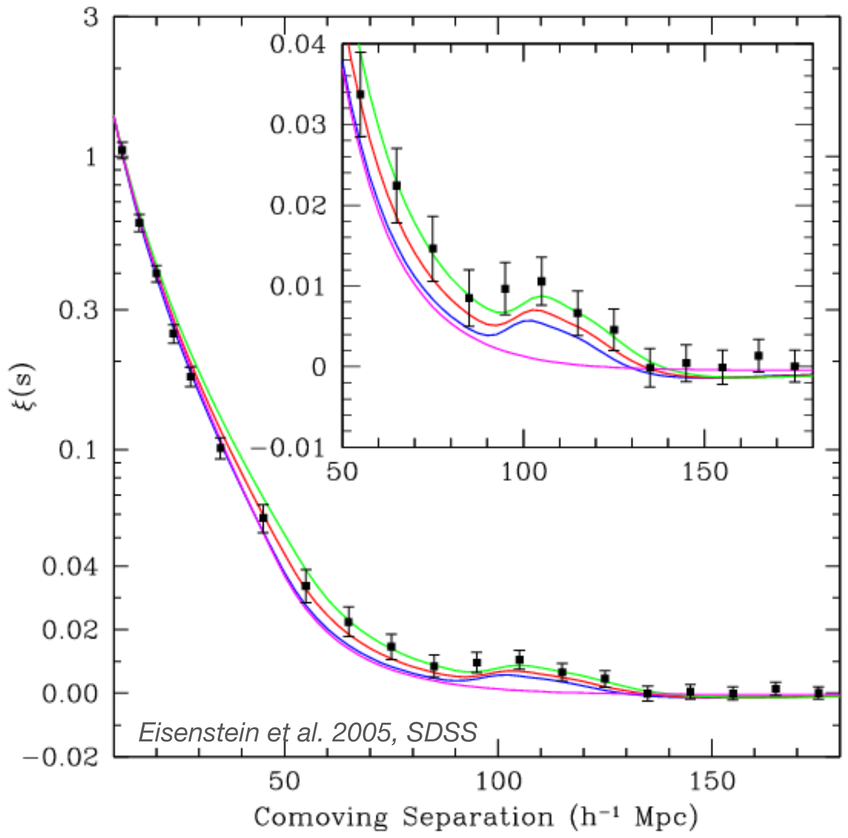

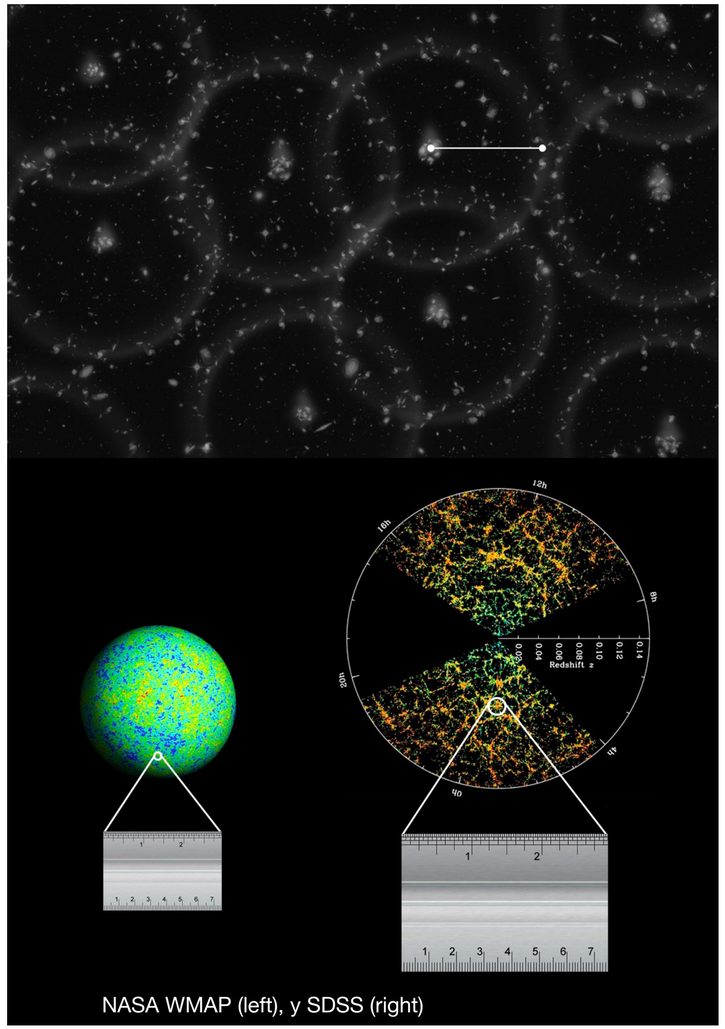

Galaxy clustering: 2pt statistics

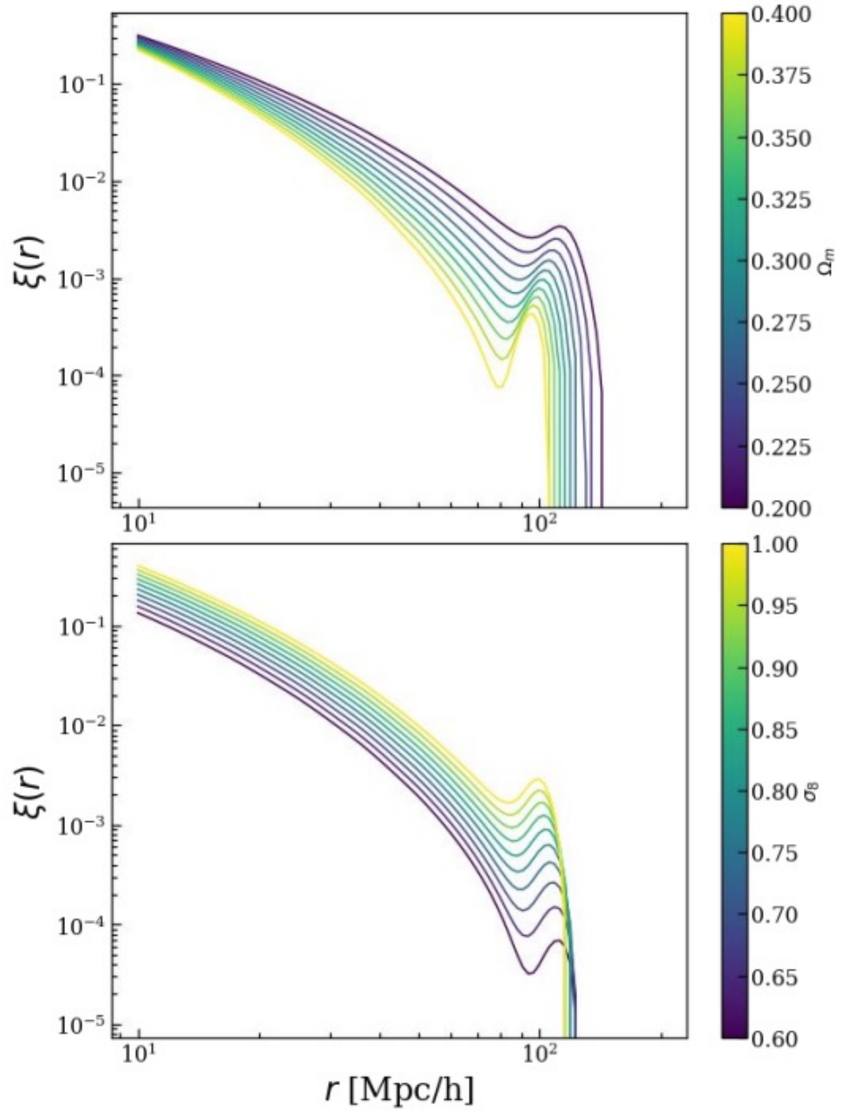

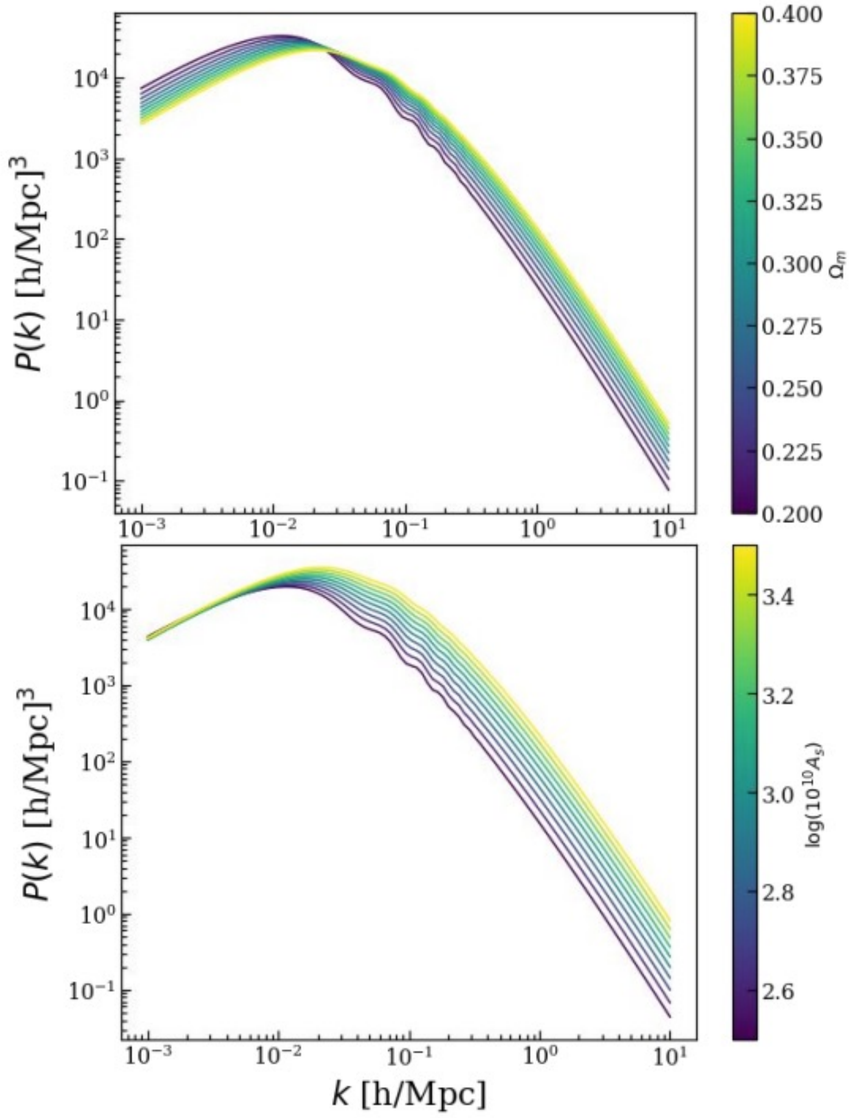

BAO in CMB and galaxy spectra

CMB temperature angular power spectra

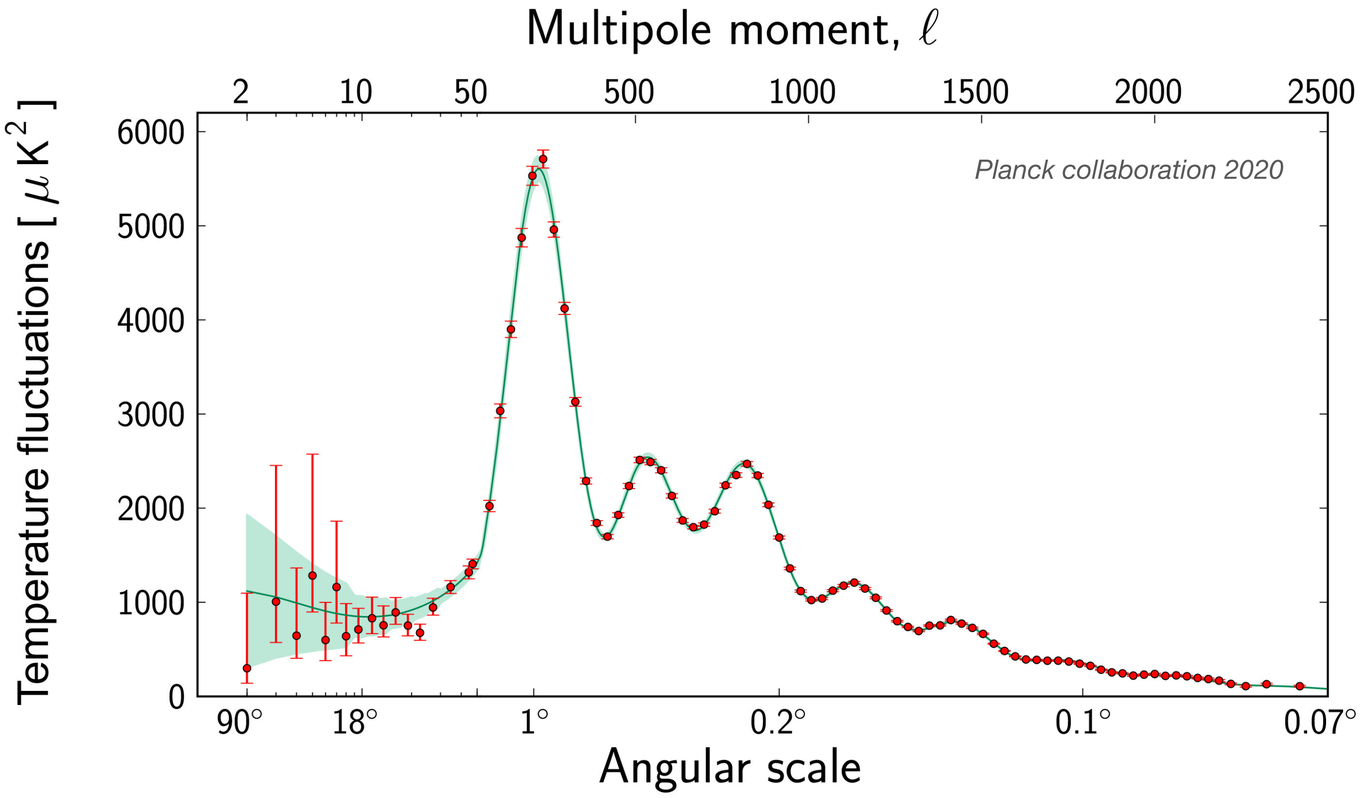

BAO signal from galaxy angular power spectra

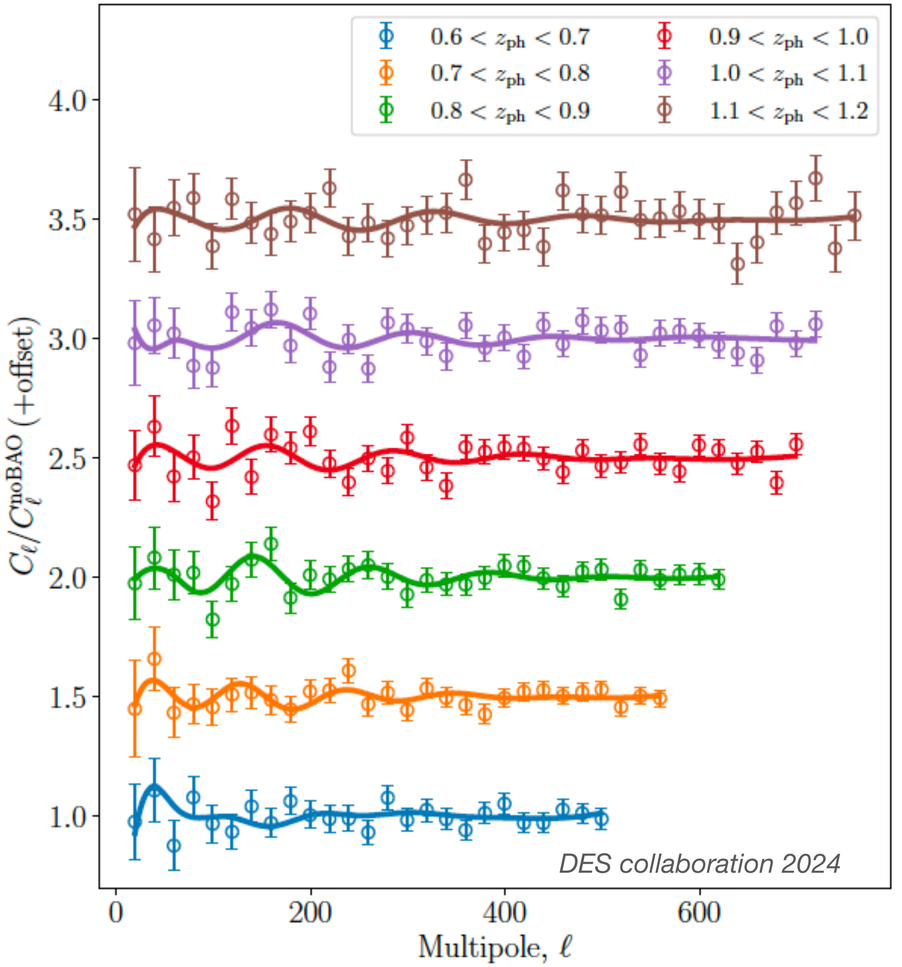

BAO as a standard ruler

This particular scale (~150 Mpc) serves as a standard ruler and is determined by the sound horizon scale of the BAO at the time of recombination

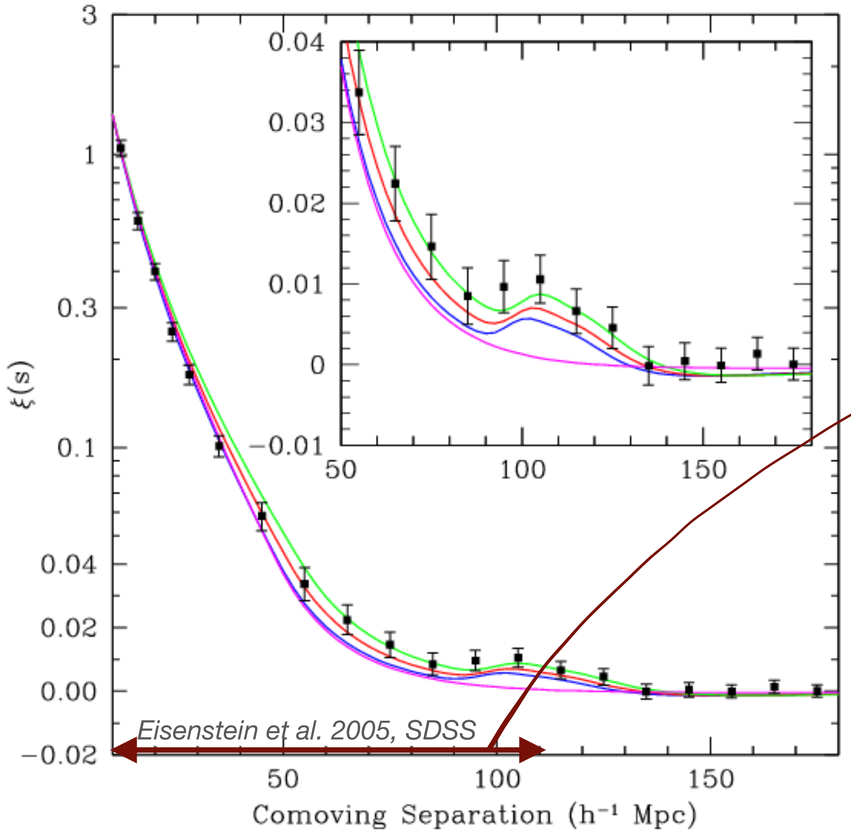

$$r_s(z_\star) = \int_{z_\star}^{\infty} \frac{c_s(z)}{H(z)}\, dz$$

$$k_{\mathrm{BAO}} = 2\pi / r_s = 0.06\ h/\mathrm{Mpc}$$

BAO as a standard ruler

In practice, **we measure angles and redshifts** from galaxy surveys and infer distances to get cosmological information

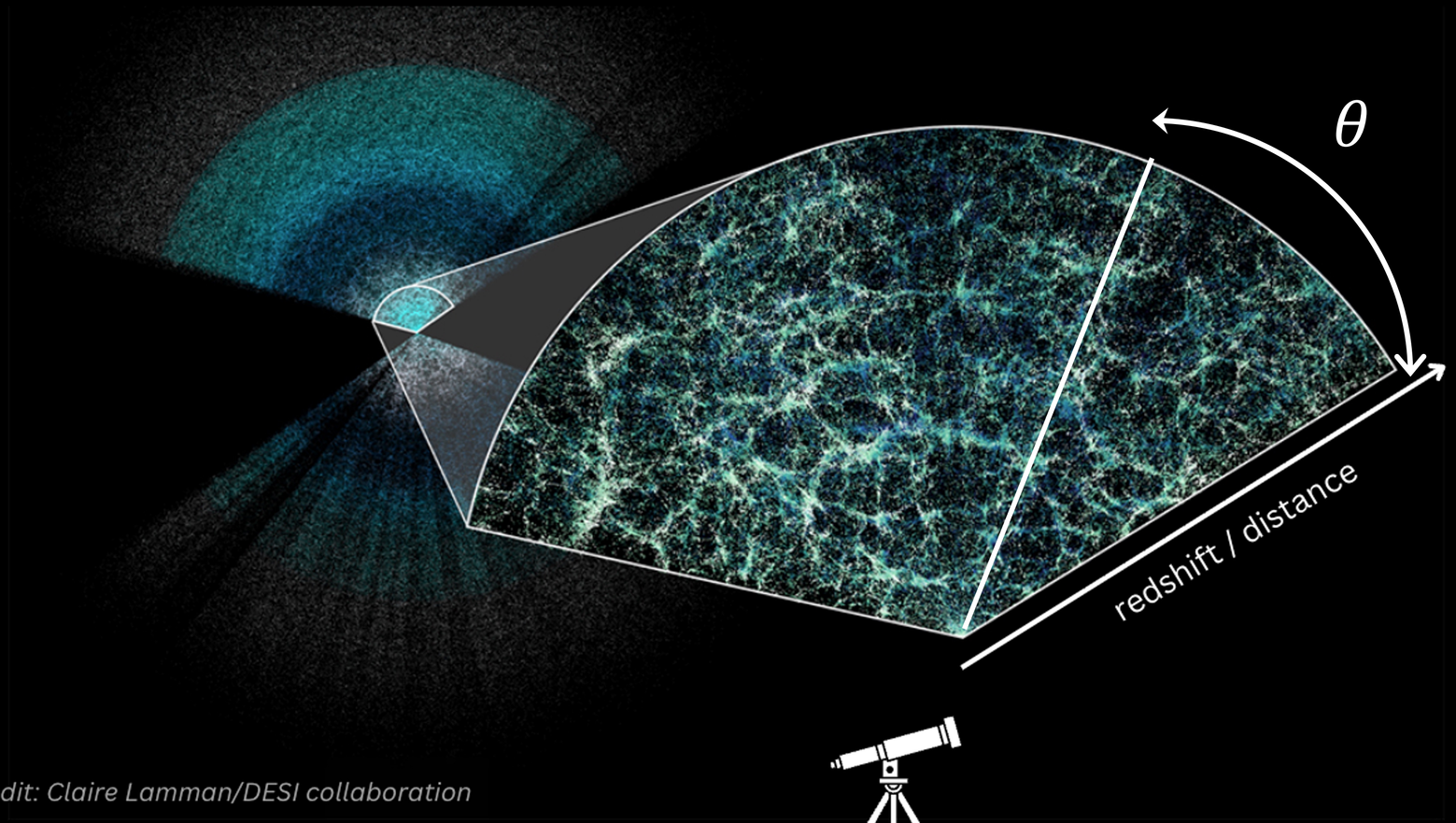

Credit: Claire Lamman/DESI collaboration

BAO as a standard ruler

In practice, **we measure angles and redshifts** from galaxy surveys and infer distances to get cosmological information

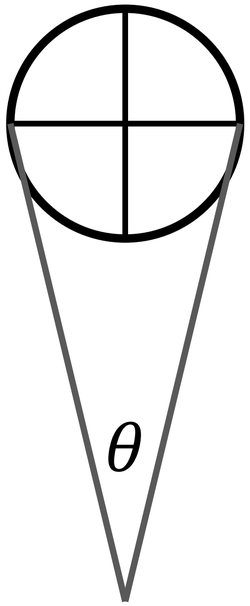

$$s_\perp(z) = d_A(z)\Delta\theta(1+z)$$

perpendicular to the line of sight

$$s_\parallel(z) = \frac{c\Delta z}{H(z)}$$

parallel to the line of sight

BAO as a standard ruler

In practice, **we measure angles and redshifts** from galaxy surveys and infer distances to get cosmological information

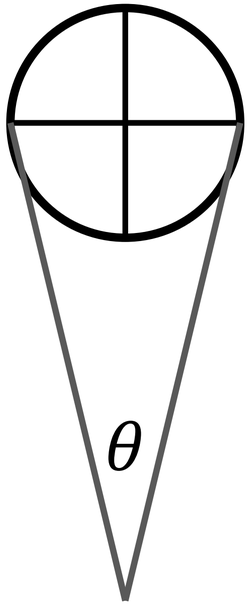

$$s_\perp(z) = d_A(z)\Delta\theta(1+z) = D_M(z)\Delta\theta$$

perpendicular to the line of sight

$$s_\parallel(z) = \frac{c\Delta z}{H(z)}$$

parallel to the line of sight

Alcock-Paczynski (AP) test: the BAO scale should be spherically symmetric in real space ($\Delta\theta = \Delta z$)

$$F_{AP}(z) \equiv \frac{\Delta z}{\Delta\theta} = \frac{H(z)D_M(z)s_\parallel(z)}{cs_\perp(z)}$$

BAO as a standard ruler

In practice, we assume a fiducial cosmological model to convert redshifts and angles to physical distances, and the AP parameters characterise this dilation

$$\alpha_{\parallel} = \frac{H^{\rm fid}(z) r_d^{\rm fid}}{H(z) r_d} \qquad \alpha_{\perp} = \frac{D_M(z) r_d^{\rm fid}}{D_M^{\rm fid}(z) r_d}$$

$$\alpha_{\rm AP} = \alpha_{\parallel} / \alpha_{\perp}$$

Also used the geometric mean, combining the radial and transverse dilations: $\alpha_{\rm iso} = \left(\alpha_{\parallel} \alpha_{\perp}^2\right)^{1/3}$

Redshift Space Distortions

There is anisotropy in the clustering observations due to the **peculiar velocities** of galaxies, which contribute to the observed redshift

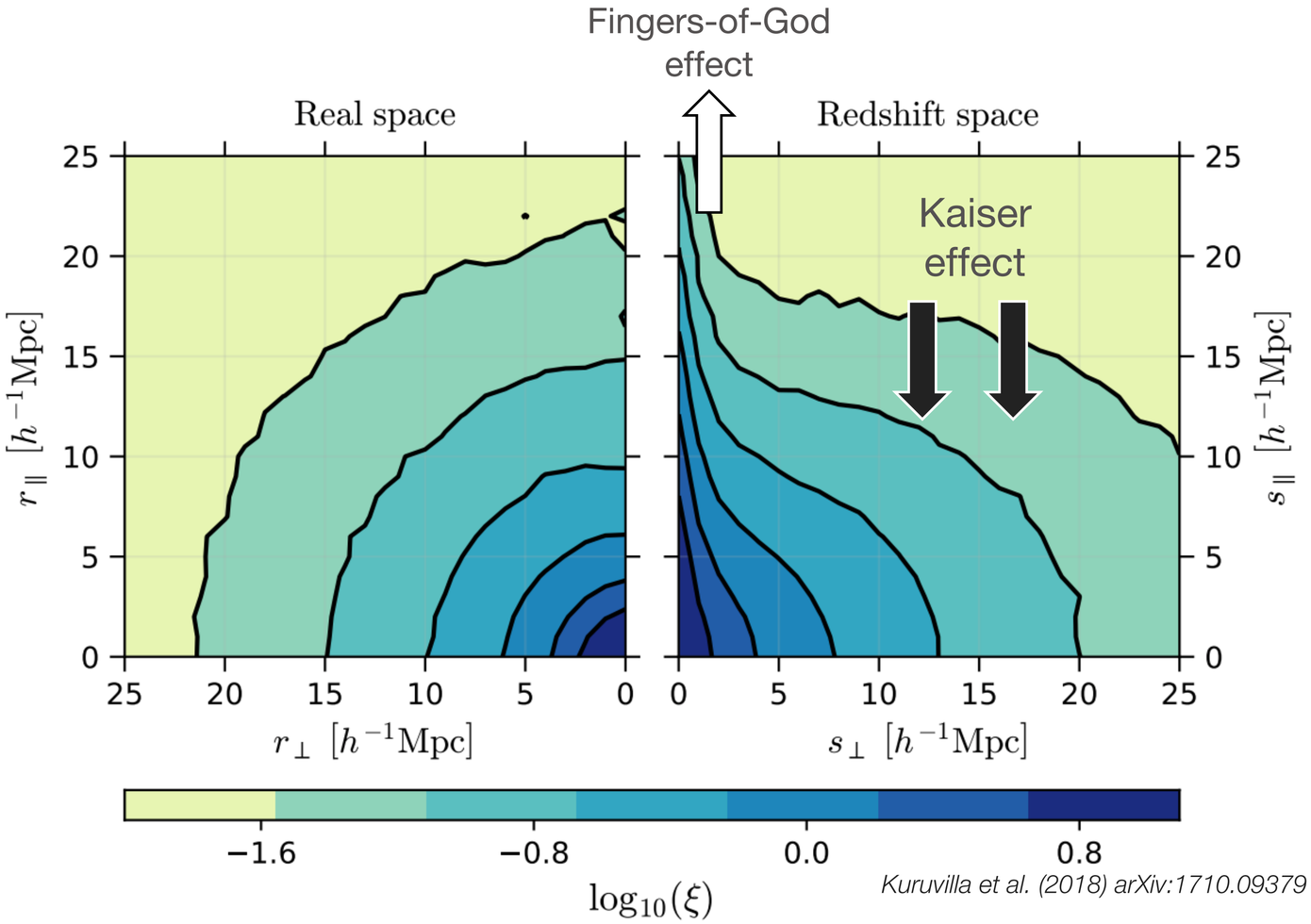

Kuruvilla et al. (2018) arXiv:1710.09379

Redshift Space Distortions

There is anisotropy in the clustering observations due to the **peculiar velocities** of galaxies, which contribute to the observed redshift

Real Space

Redshift Space

Peculiar velocities are small compared to the Hubble flow

Linear

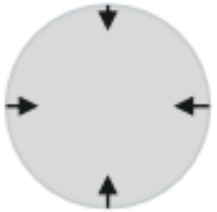

Power is enhanced at large scales

Peculiar velocities are large

Non Linear

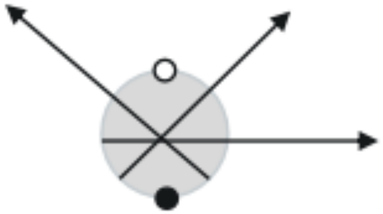

Power is suppressed at small scales

Anisotropic clustering

Besides measuring the correlation function in parallel and transverse separations, we can decompose the power spectrum or correlation function into multipoles

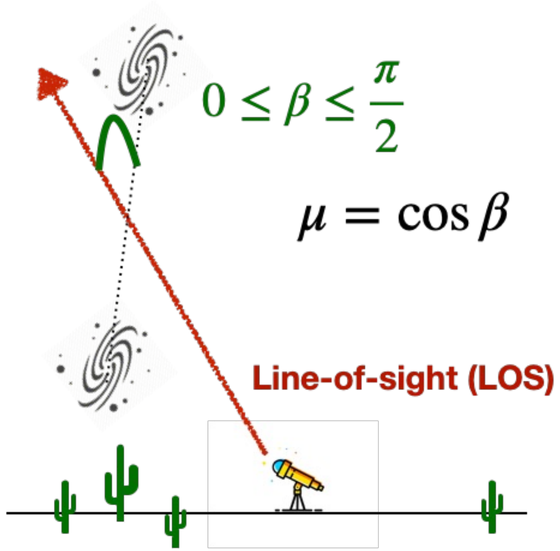

Credit figure: H. Gil-Marín

In the linear regime, the redshift space power spectrum is given by the Kaiser factor

$$P_g^{(s)}(k,\mu) = \left[b + f\mu^2\right]^2 P_m(k) \qquad f(z) = \frac{\mathrm{d}\ln D}{\mathrm{d}\ln a}$$

$$P^{(s)}(k,\mu) = \underbrace{P^{(0)}(k)L_0(\mu)}_{\text{monopole}} + \underbrace{P^{(2)}(k)L_2(\mu) + P^{(4)}(k)L_4(\mu)}_{\text{quadrupole} \quad \text{hexadecapole}}$$

Isotropic signal — Anisotropic signal

Anisotropic clustering

$$P^{(s)}(k,\mu) = \underbrace{P^{(0)}(k)L_0(\mu)}_{\text{monopole}} + \underbrace{P^{(2)}(k)L_2(\mu) + P^{(4)}(k)L_4(\mu)}_{\text{quadrupole}\quad\text{hexadecapole}}$$

Isotropic signal — Anisotropic signal

$$P^{(0)}(k,z) = \left(b(z)^2 + \frac{2}{3} b(z) f(z) + \frac{1}{5} f(z)^2 \right) P_m(k,z)$$

$$P^{(2)}(k,z) = \left(\frac{4}{3} b(z) f(z) + \frac{4}{7} f(z)^2 \right) P_m(k,z)$$

$$P^{(4)}(k,z) = \left(\frac{8}{35} f(z)^2 \right) P_m(k,z)$$

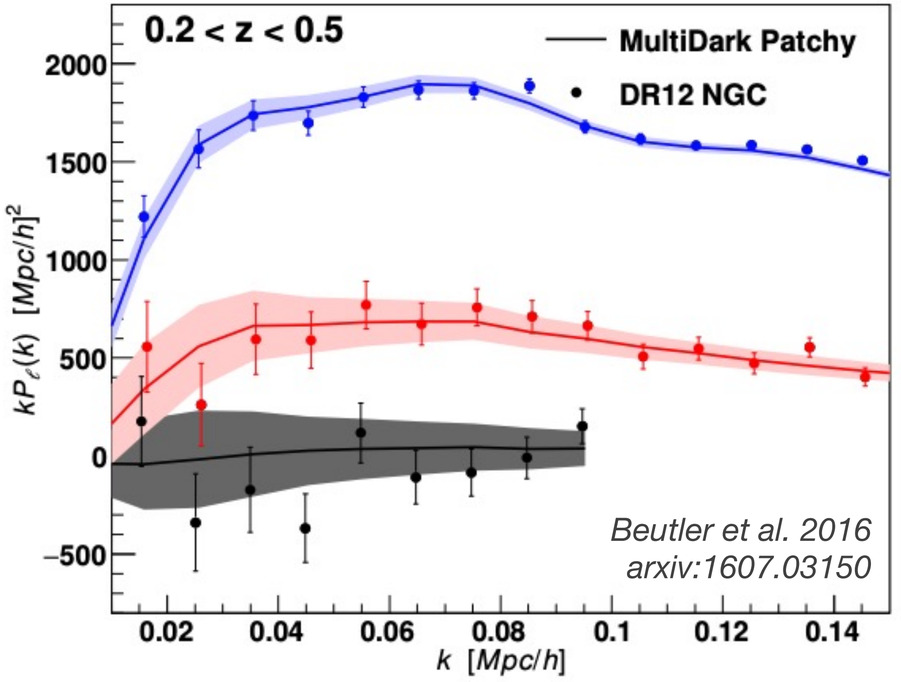

Anisotropic clustering

$$P^{(s)}(k,\mu) = \underbrace{P^{(0)}(k)L_0(\mu)}_{\text{monopole}} + \underbrace{P^{(2)}(k)L_2(\mu) + P^{(4)}(k)L_4(\mu)}_{\text{quadrupole}\qquad\text{hexadecapole}}$$

Isotropic signal — Anisotropic signal

$$P^{(0)}(k,z) = \left(b(z)^2 + \frac{2}{3}b(z)f(z) + \frac{1}{5}f(z)^2\right)P_m(k,z)$$

$$P^{(2)}(k,z) = \left(\frac{4}{3}b(z)f(z) + \frac{4}{7}f(z)^2\right)P_m(k,z)$$

$$P^{(4)}(k,z) = \left(\frac{8}{35}f(z)^2\right)P_m(k,z)$$

$$\sigma_8(z) = \sigma_8(z=0)\frac{D(z)}{D(z=0)}$$

$$P_m(k,z) = \sigma_8(z)P_m(k,z=0)$$

We can constrain $b(z)\sigma_8(z)$ & $f(z)\sigma_8(z)$

BAO damping

Smoothing of the BAO peak/wiggles due to the effects of non-linear clustering (incl. RSD) reduces our ability to measure the BAO scale

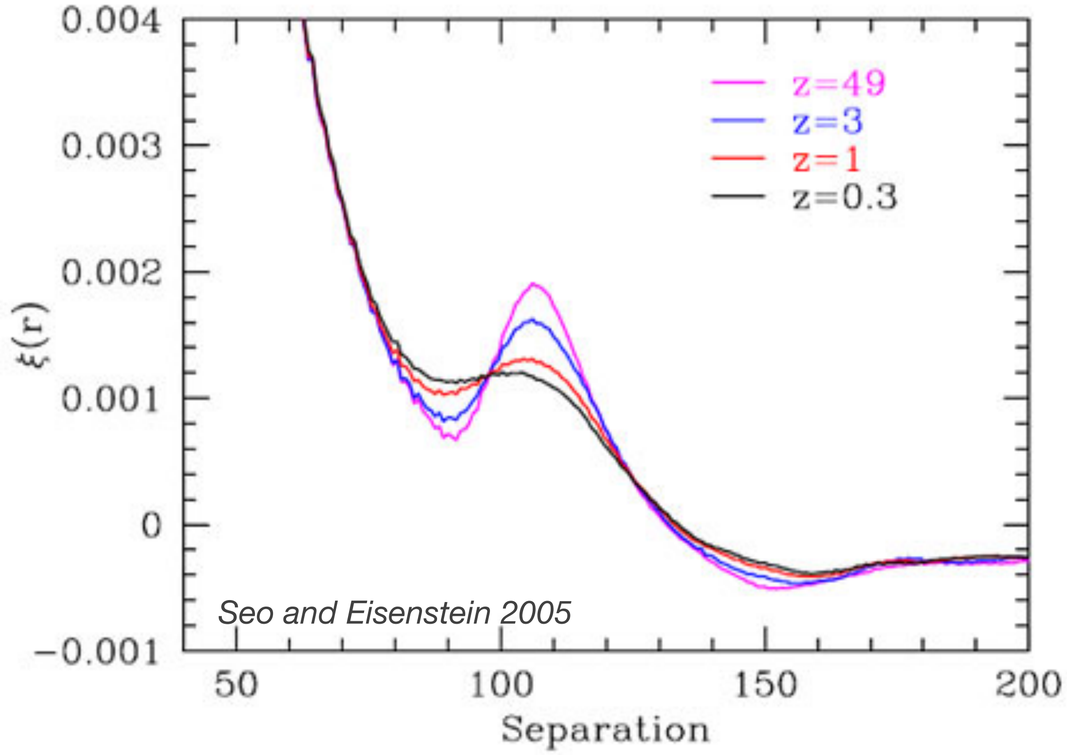

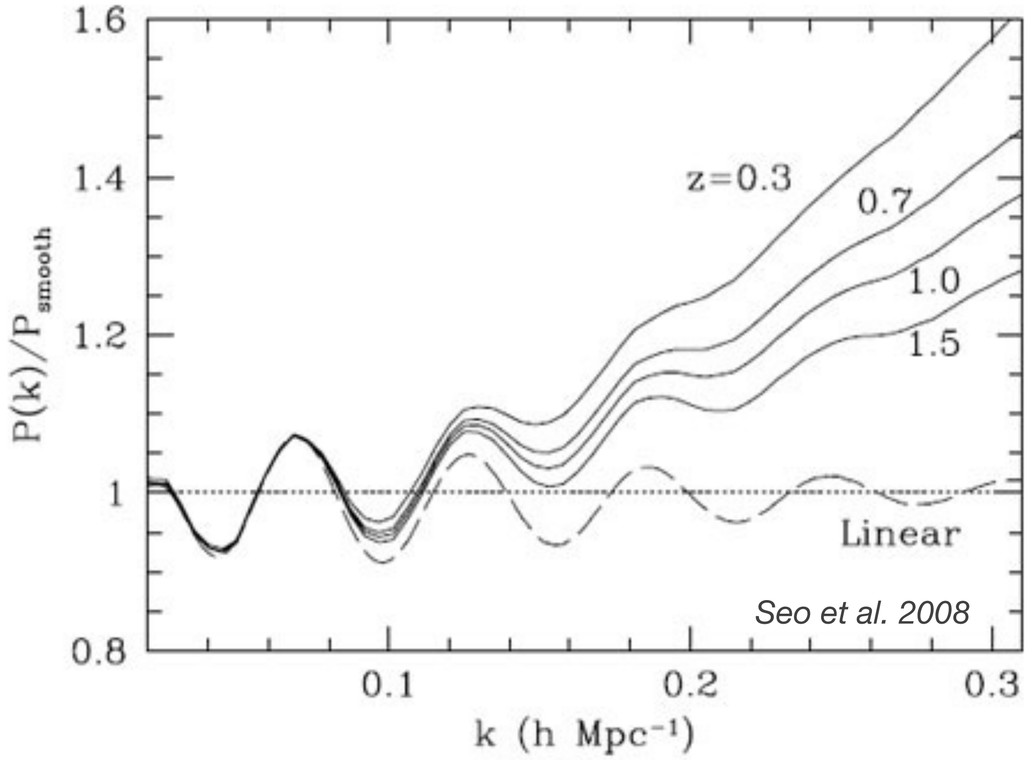

BAO reconstruction

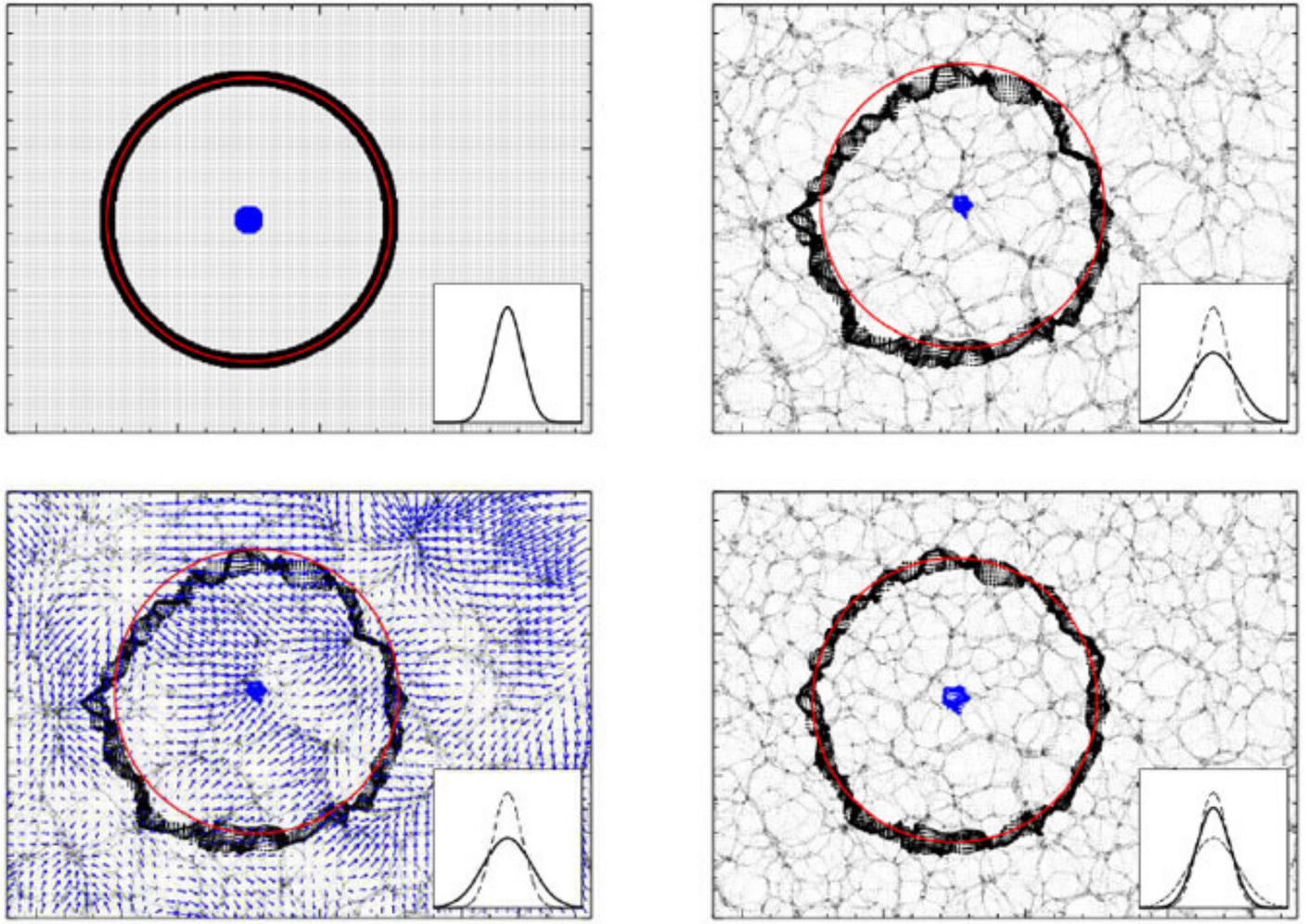

Padmanabhan et al. (2012)

The idea is to estimate the displacement field from the final density field and then move the particles back to their initial positions (reverse the displacement)

BAO reconstruction

The dominant non-linear effect responsible for the BAO damping is the large-scale velocity field. In particular, the motions are dominantly due to bulk flows and the formation of superclusters.

Simple algorithm: smooth the density field and move the overdensities by the inverse of the predicted (linear) motion

Eisenstein et al. 2006; arxiv:0604362

BAO reconstruction

The dominant non-linear effect responsible for the BAO damping is the large-scale velocity field. In particular, the motions are dominantly due to bulk flows and the formation of superclusters.

Simple algorithm: smooth the density field and move the overdensities by the inverse of the predicted (linear) motion

to remove small-scale information

Eisenstein et al. 2006; arxiv:0604362

BAO reconstruction

The dominant non-linear effect responsible for the BAO damping is the large-scale velocity field. In particular, the motions are dominantly due to bulk flows and the formation of superclusters.

Simple algorithm: smooth the density field and move the overdensities by the inverse of the predicted (linear) motion

Several improved reconstruction algorithms in the literature: Seo et al 2010, Schmittfull et al. 2017, Hada et al. 2018

The method is now well tested. If the reconstruction is off, it usually impacts the efficiency of the reconstruction, not the measurement

Eisenstein et al. 2006; arxiv:0604362

BAO reconstruction

One can also use the estimate of the large-scale displacements to remove large-scale redshift-space distortions

Padmanabhan et al. (2012)

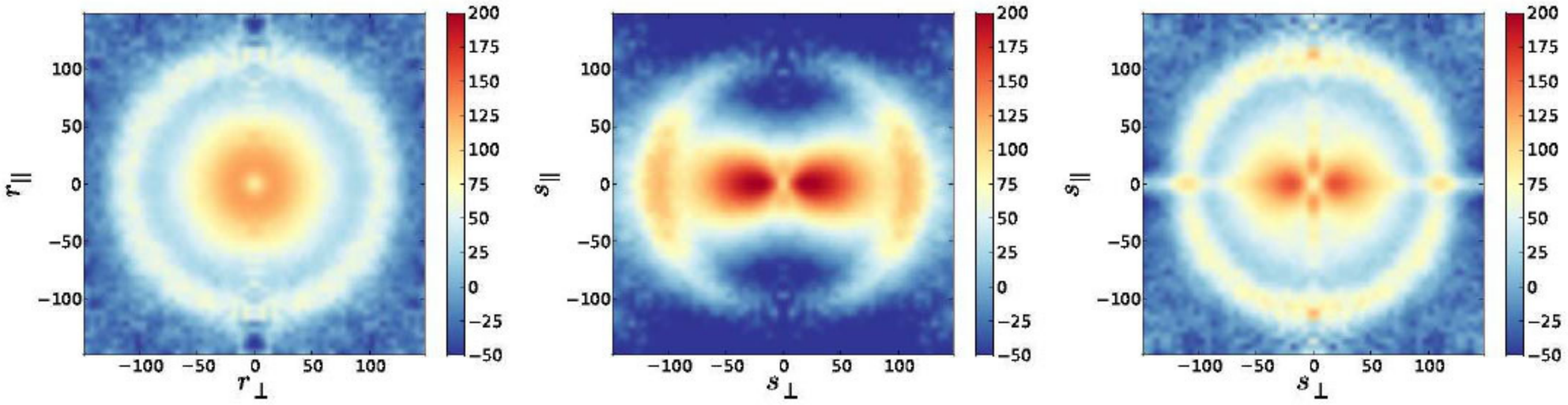

Real space

Redshift space pre-reconstruction

Redshift space post-reconstruction

Example from DESI DR1

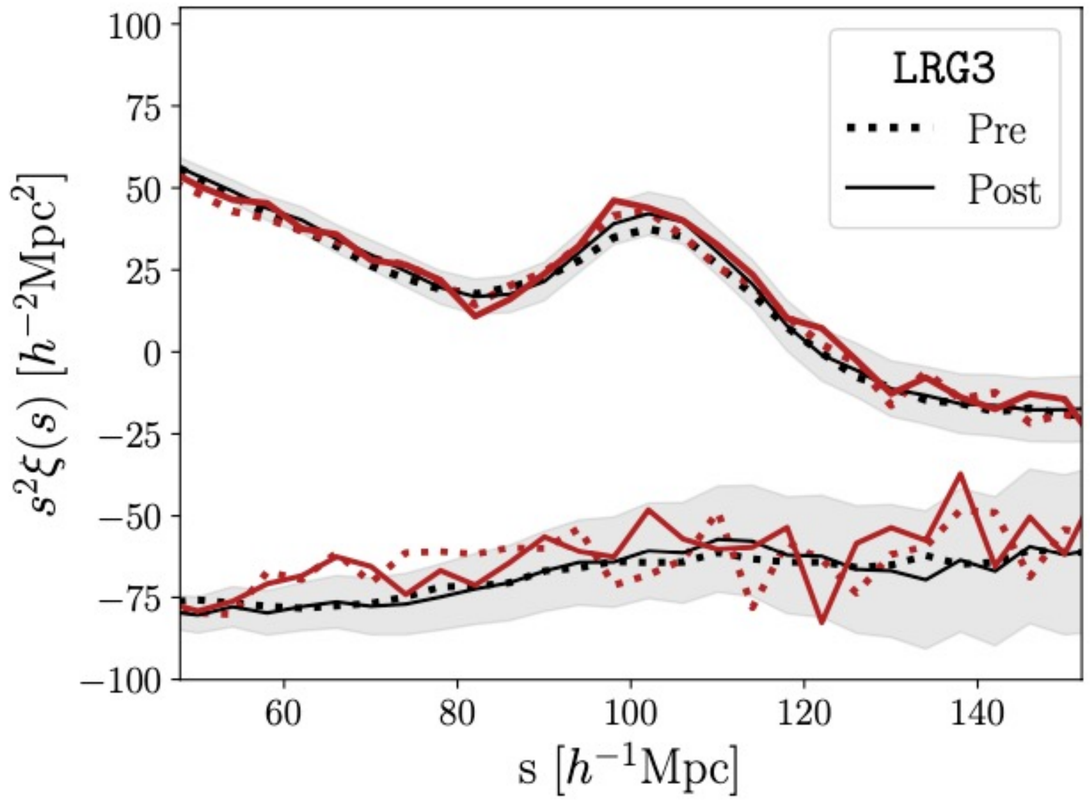

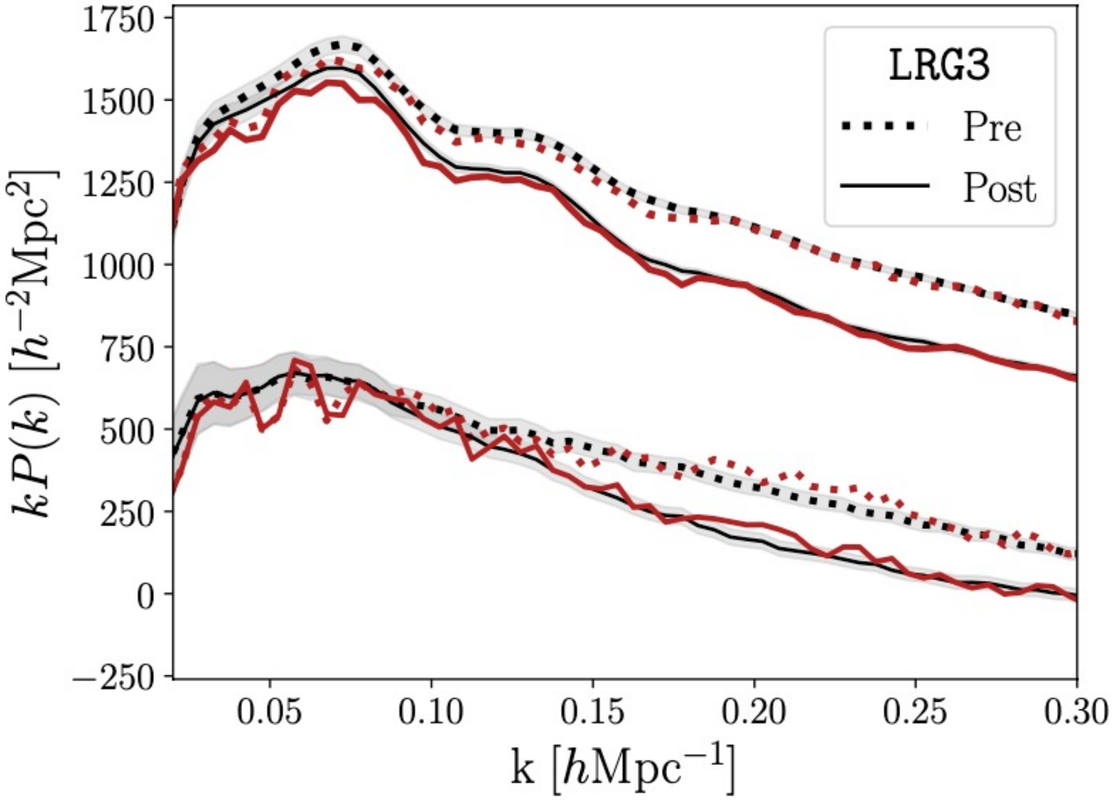

DESI collaboration 2024; arxiv:2404.03000

BAO fitting

We use as template the predicted clustering for the assumed cosmological model to isolate the BAO signal

In practice, the template is modified to allow for effects of non-linear structure formation and includes broad-band terms (to be marginalized over) that account for scale-dependent bias or calibration errors

$$P_{\rm measure}(k) = B(k) P_m(k/\alpha) + A(k)$$

BAO fitting

We use as template the predicted clustering for the assumed cosmological model to isolate the BAO signal

In practice, the template is modified to allow for effects of non-linear structure formation and includes broad-band terms (to be marginalized over) that account for scale-dependent bias or calibration errors

$$P_{\rm measure}(k) = B(k)P_m(k/\alpha) + A(k)$$

Smooth functions with nuisance parameters to marginalize out the broadband shape of the power spectrum

BAO fitting

We use as template the predicted clustering for the assumed cosmological model to isolate the BAO signal

In practice, the template is modified to allow for effects of non-linear structure formation and includes broad-band terms (to be marginalized over) that account for scale-dependent bias or calibration errors

$$P_{\rm measure}(k) = B(k)P_m(k/\alpha) + A(k)$$

scale dilation parameter
used to adjust the location
of the BAO peak/scale

BAO fitting

We use as template the predicted clustering for the assumed cosmological model to isolate the BAO signal

In practice, the template is modified to allow for effects of non-linear structure formation and includes broad-band terms (to be marginalized over) that account for scale-dependent bias or calibration errors

$$P_{\rm measure}(k) = B(k) P_m(k/\alpha) + A(k)$$

$$P_m(k) = (P_{\rm lin}(k) - P_{\rm nw}(k)) \exp(-k^2 \Sigma_{\rm nl}) + P_{\rm nw}(k)$$

The linear power spectrum is split into a no-wiggle (nw) and a wiggle component, which is smoothed to account for the BAO damping

BAO fitting: DESI DR1

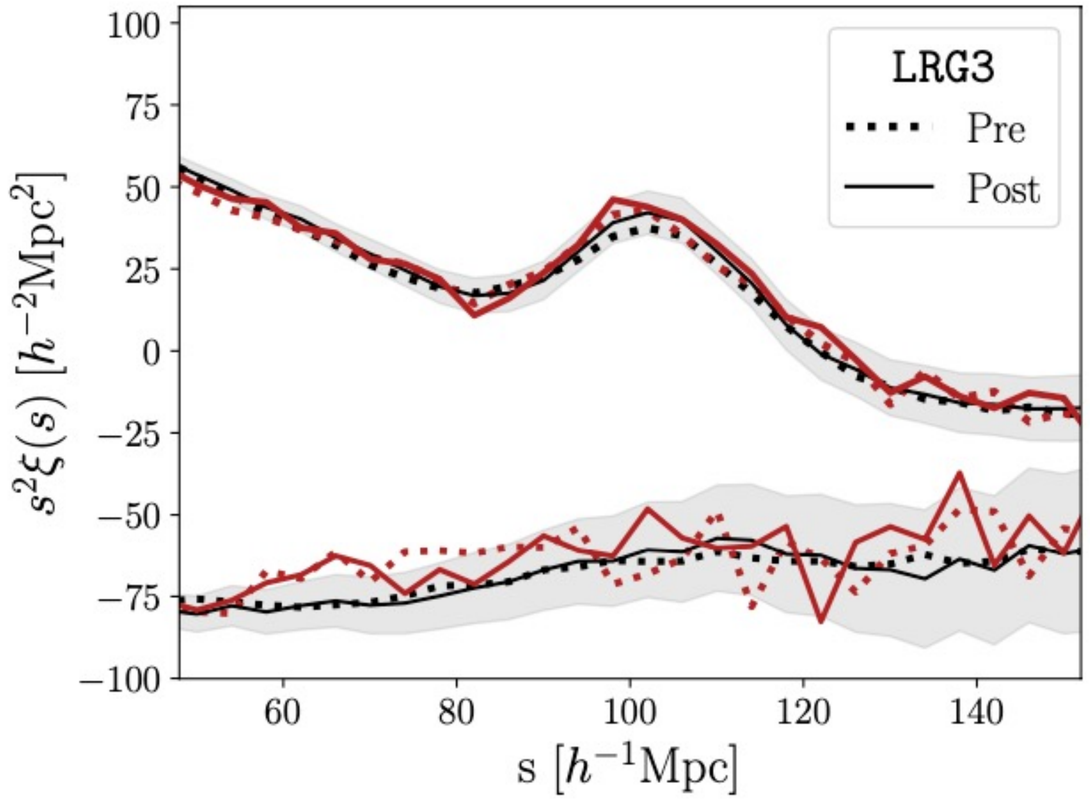

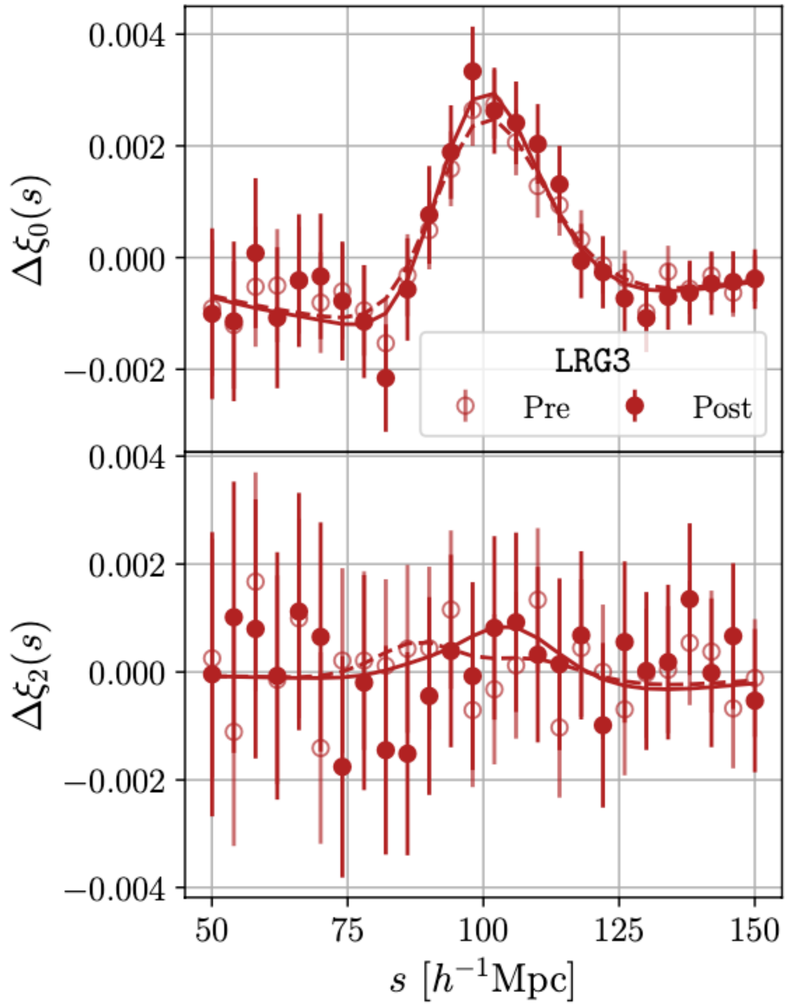

DESI collaboration 2024; arxiv:2404.03000

BAO fitting: DESI DR1

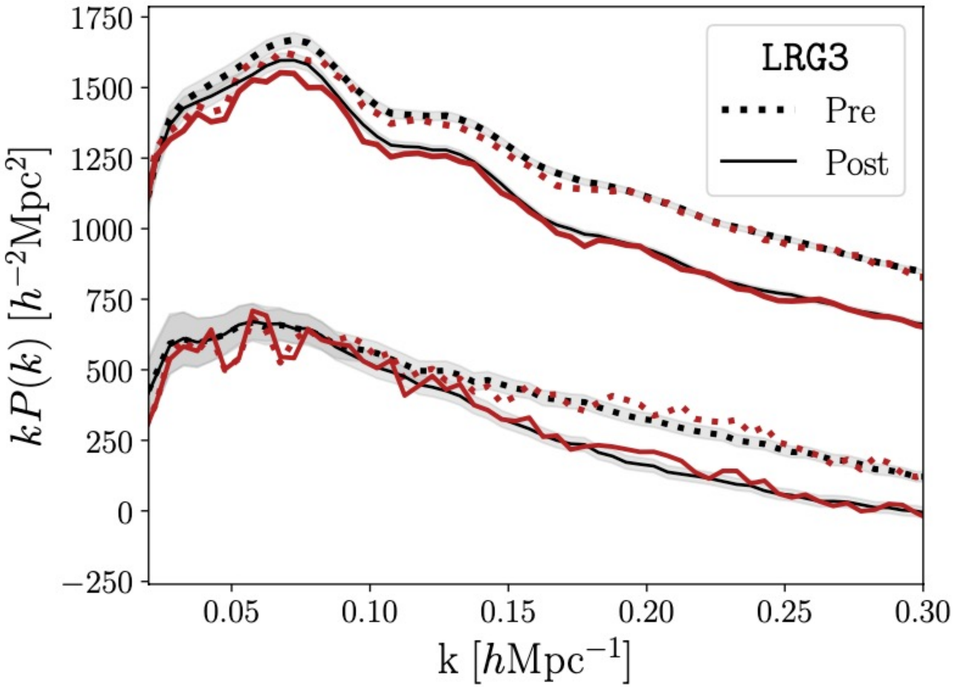

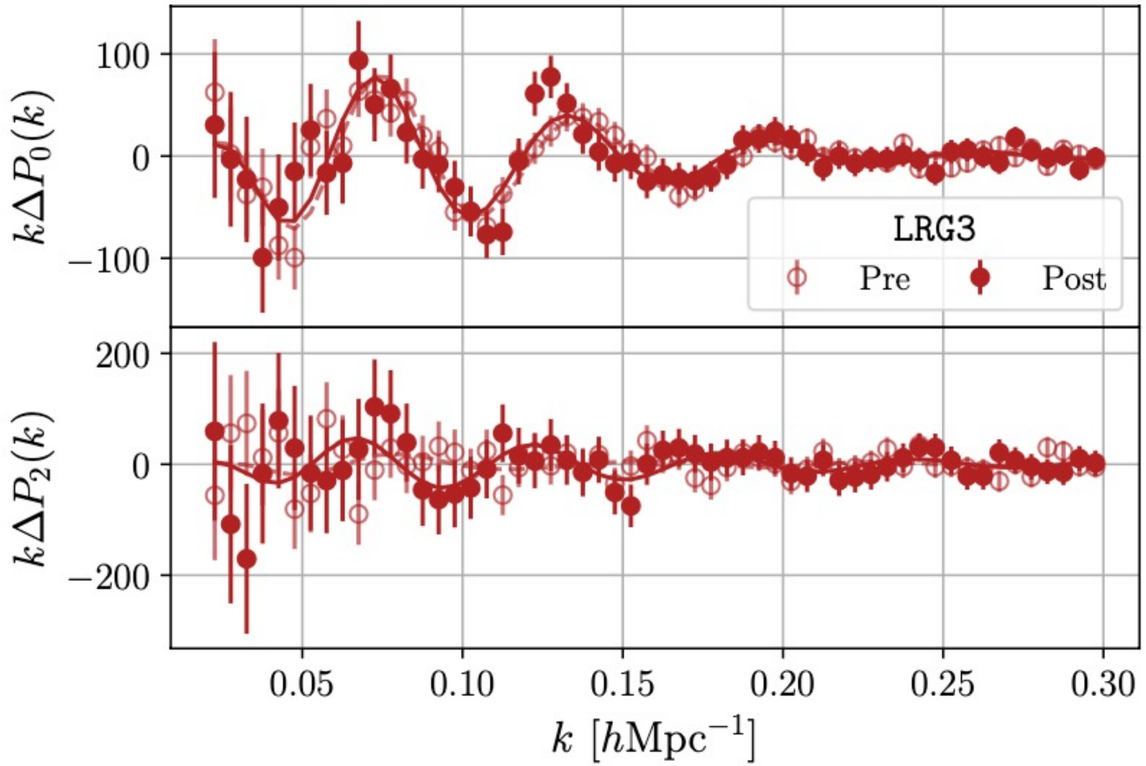

DESI collaboration 2024; arxiv:2404.03000

The Dark Energy Spectroscopic Instrument

Dark Energy Spectroscopic Instrument

Stage IV 5-year spectroscopic survey using the Mayall 4-meter telescope at Kitt Peak National Observatory, Arizona (USA)

The DESI survey started in May 2021 and just finished the first 5 years of observations

The instrument has **5000 robotically-controlled optical fibres**. In total, it's expected to catalogue redshifts from over **60 million galaxies** in 8 years, covering 17,000 sq. deg.

Image credit: DESI

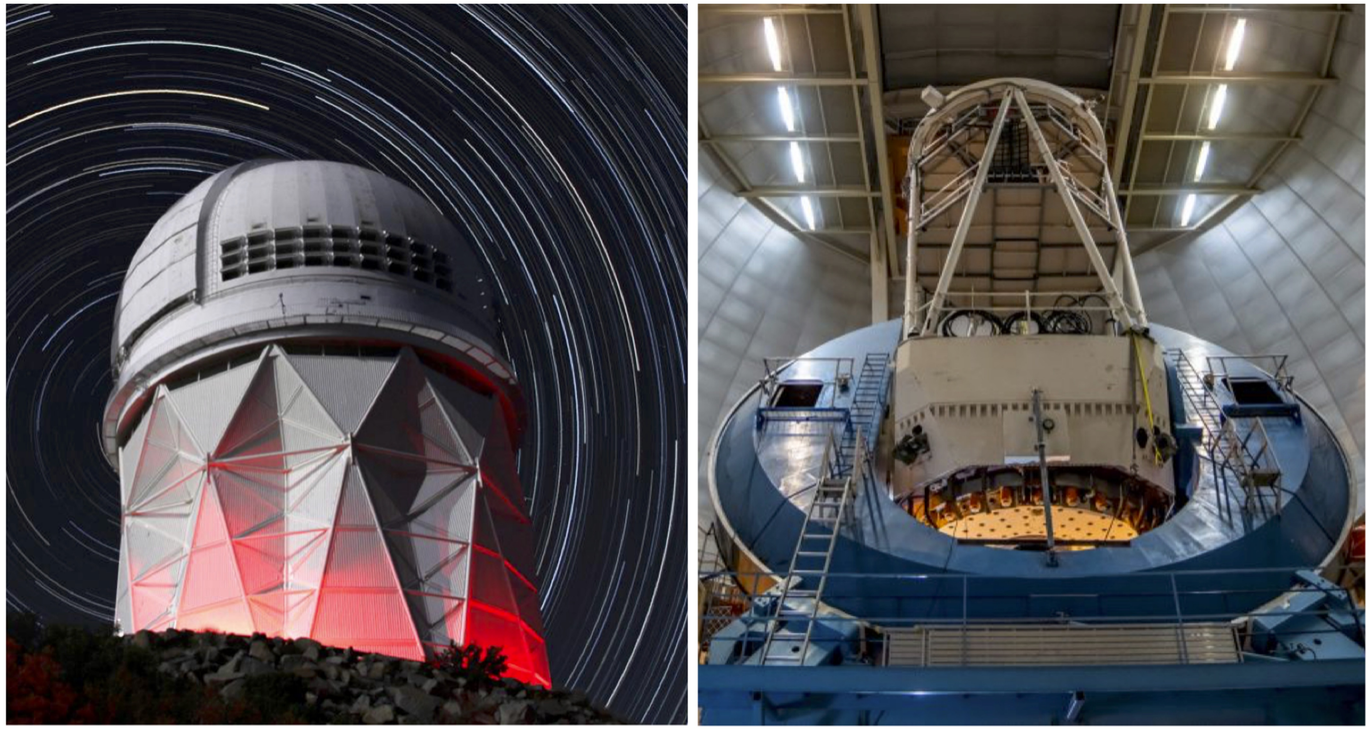

4m Mayall at Kitt Peak, Arizona. Twin to the Blanco, CTIO

Dark Energy Spectroscopic Instrument

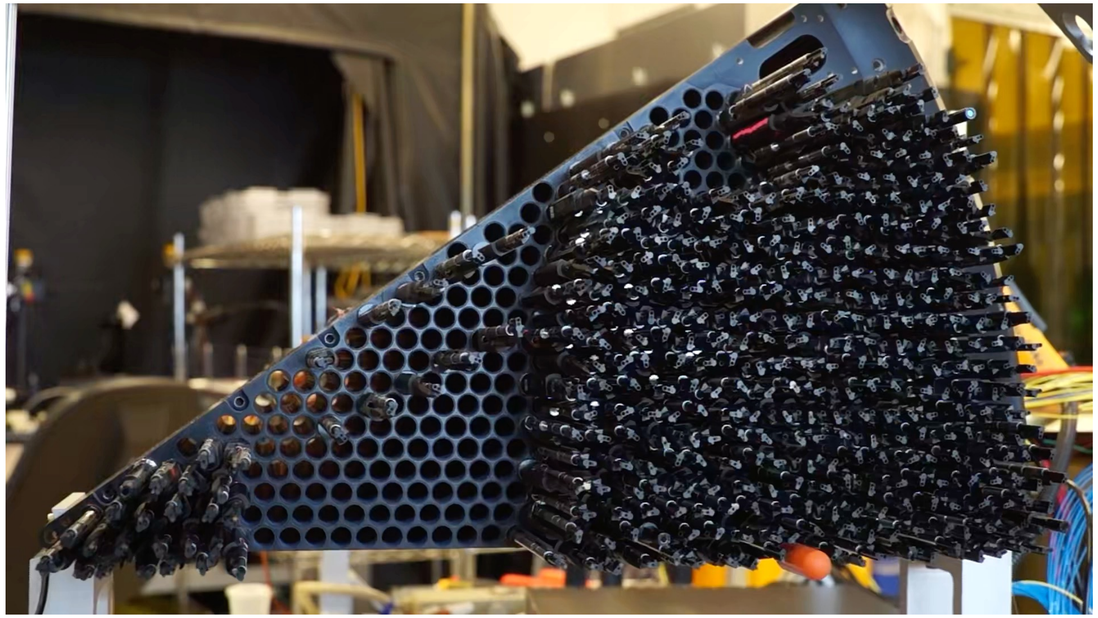

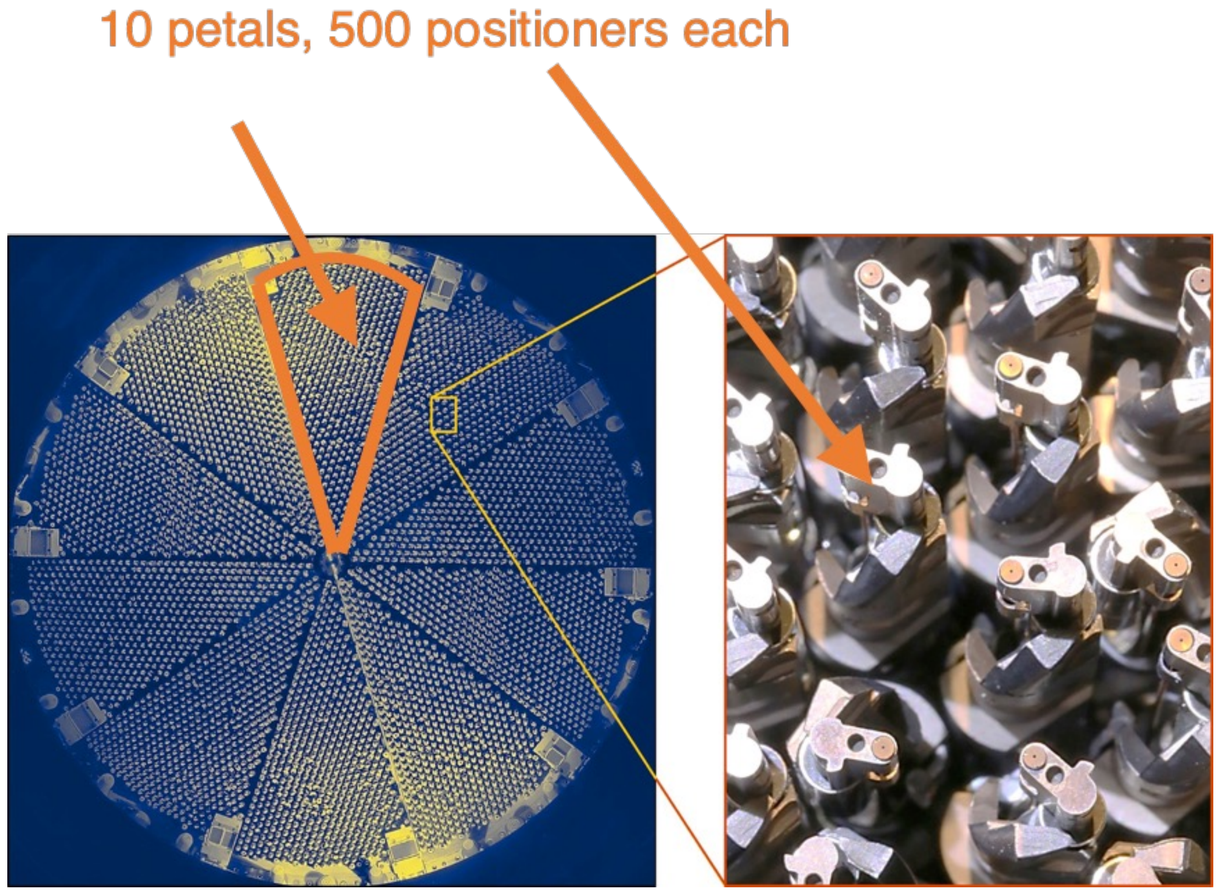

How are redshfits measured?

Each fiber positioner captures the spectra of the target galaxy

$$z = \frac{\lambda_{\text{obs.}} - \lambda_{\text{emi.}}}{\lambda_{\text{emi.}}}$$

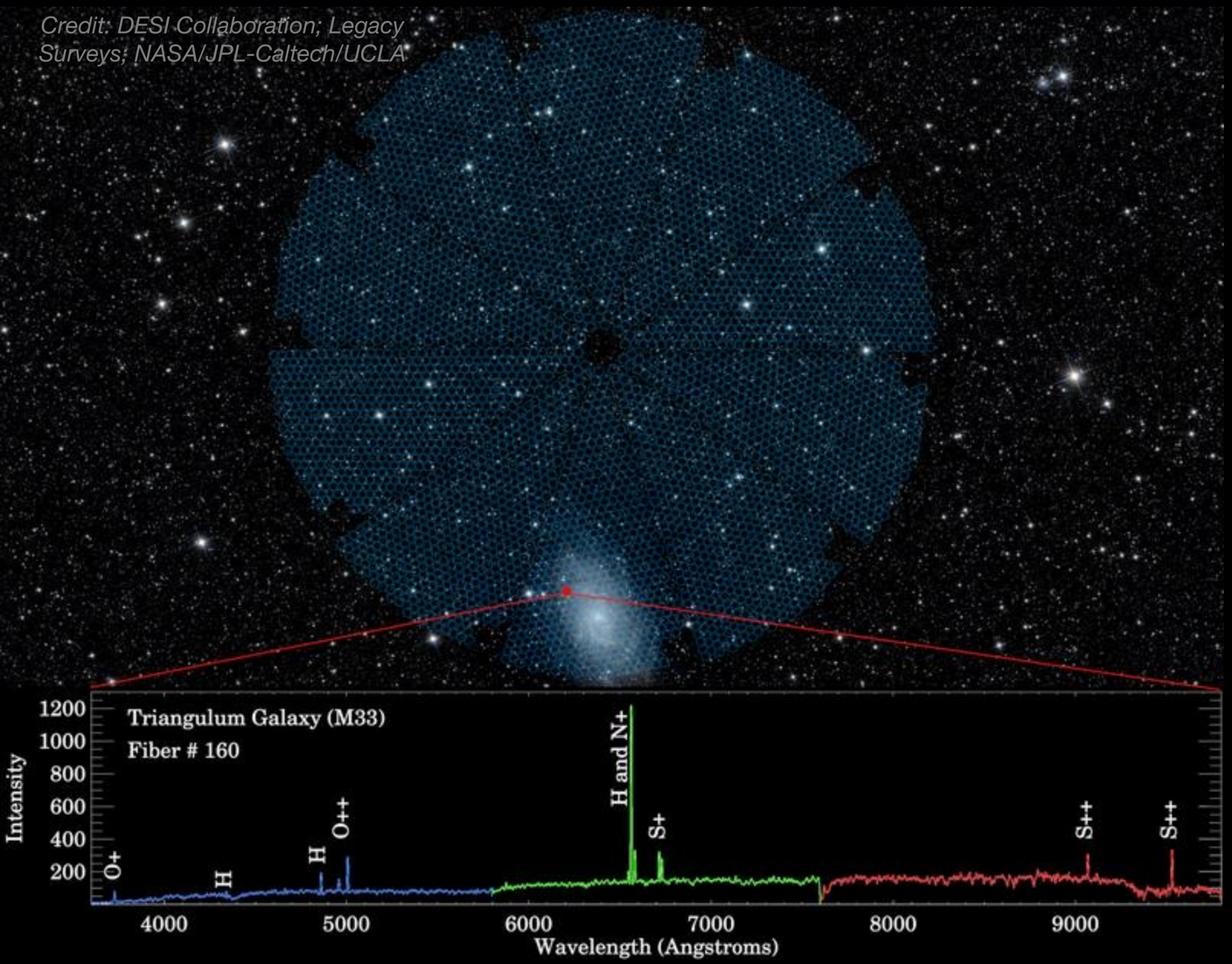

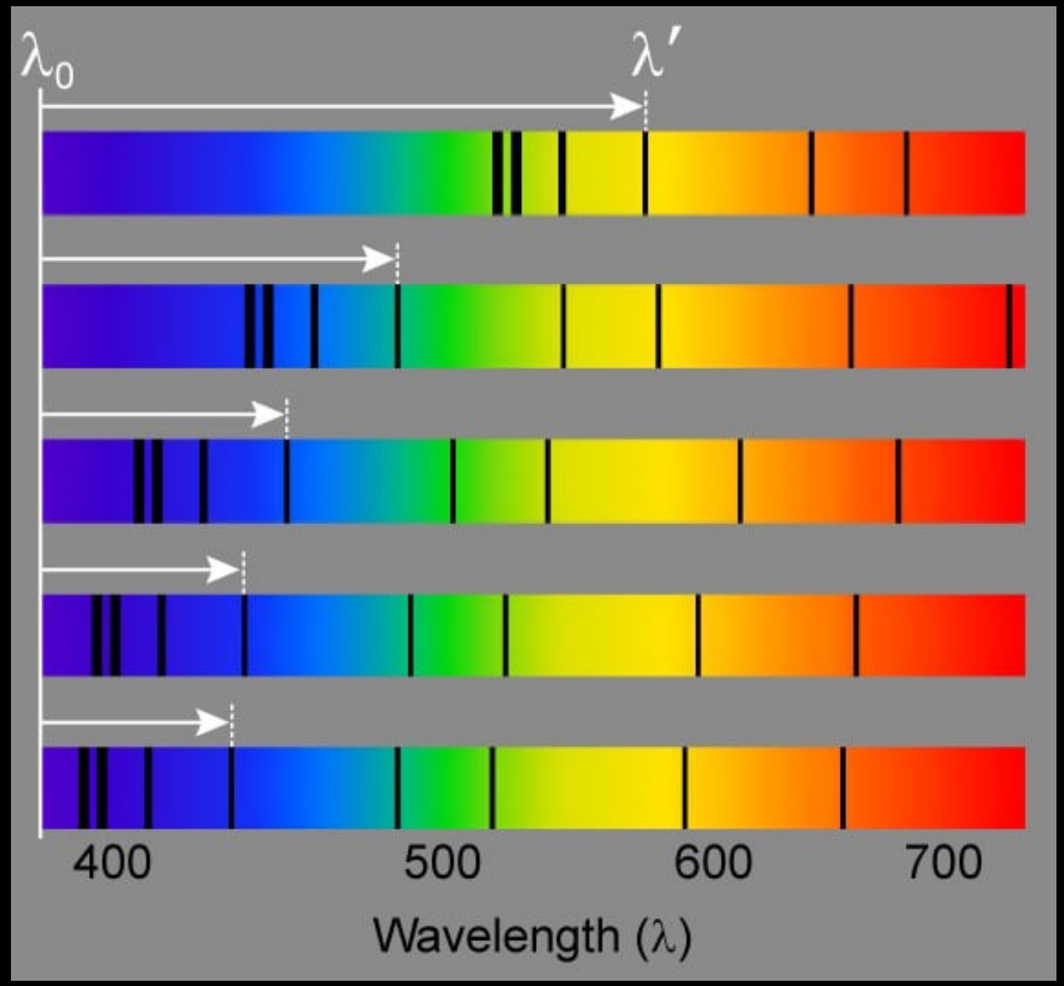

DESI Data Release 1

DESI collaboration 2025
https://arxiv.org/abs/2503.14745

DR1: 13.1M galaxy redshifts released in March 2025

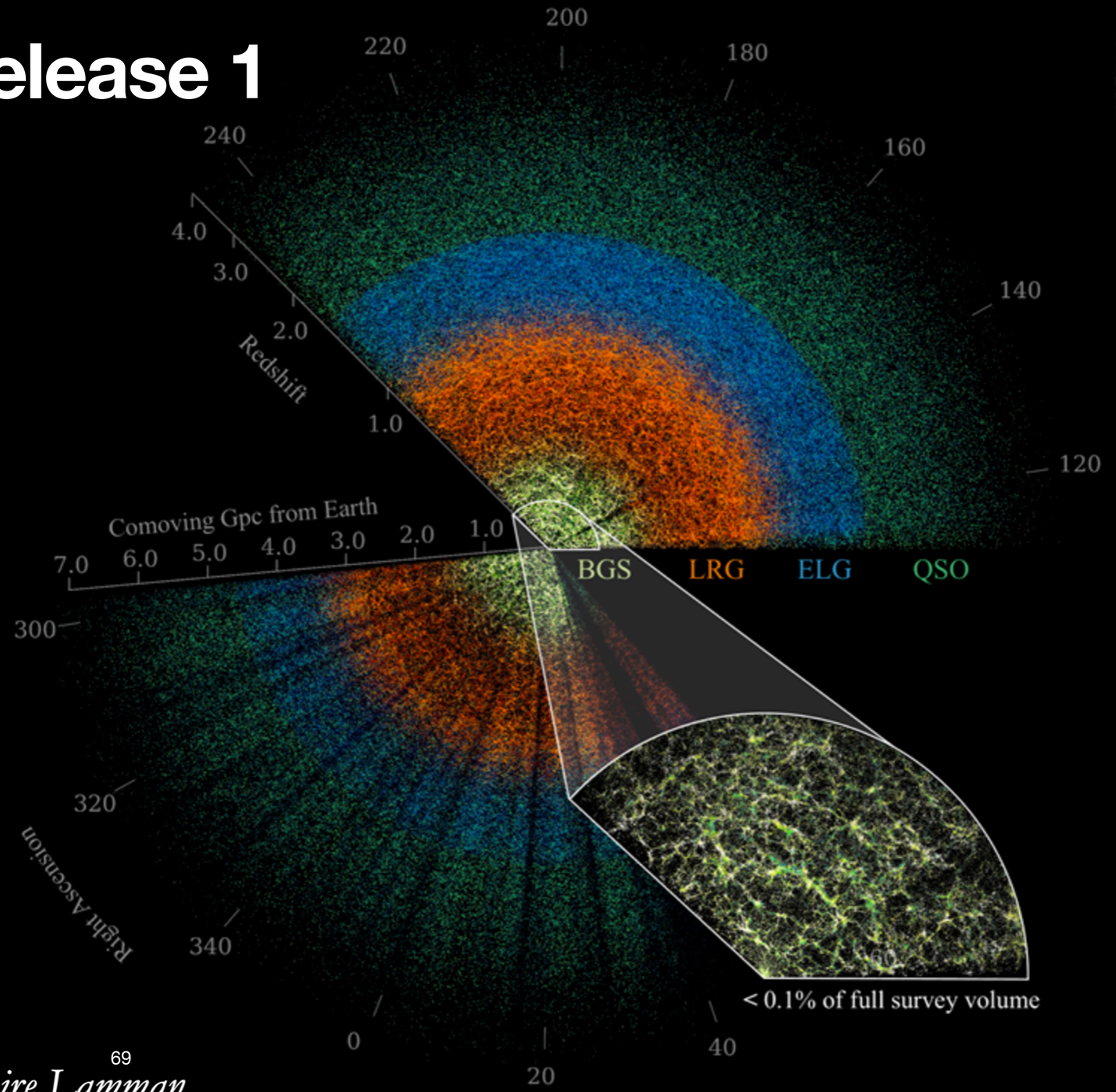

Credit: Claire Lamman

DARK ENERGY SPECTROSCOPIC INSTRUMENT

U.S. Department of Energy Office of Science

DESI DR1 footprint and coverage

DARK ENERGY SPECTROSCOPIC INSTRUMENT

U.S. Department of Energy Office of Science

First year of observations

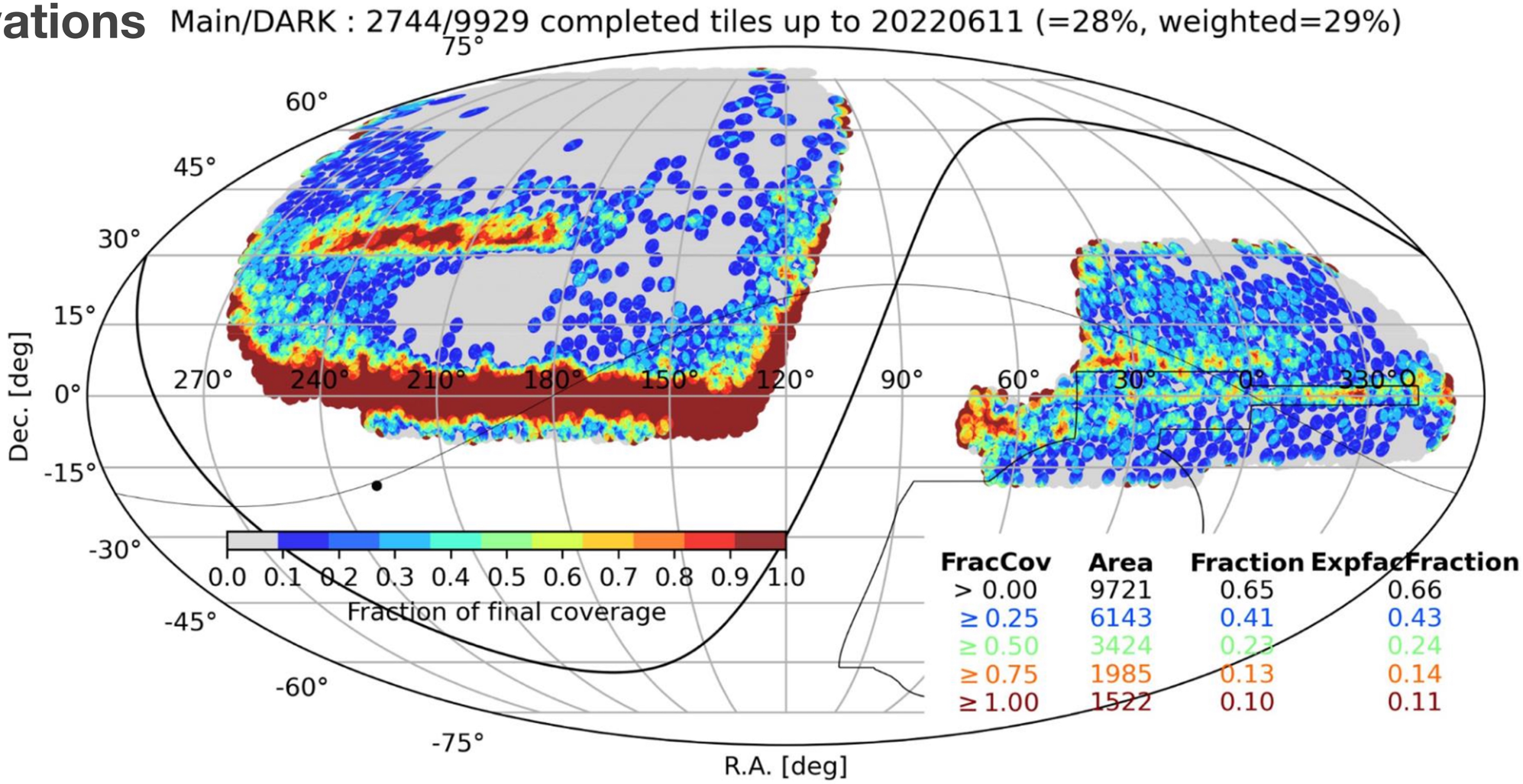

Image credi

DESI DR2 footprint and coverage

DARK ENERGY SPECTROSCOPIC INSTRUMENT

U.S. Department of Energy Office of Science

First 3 years of observations

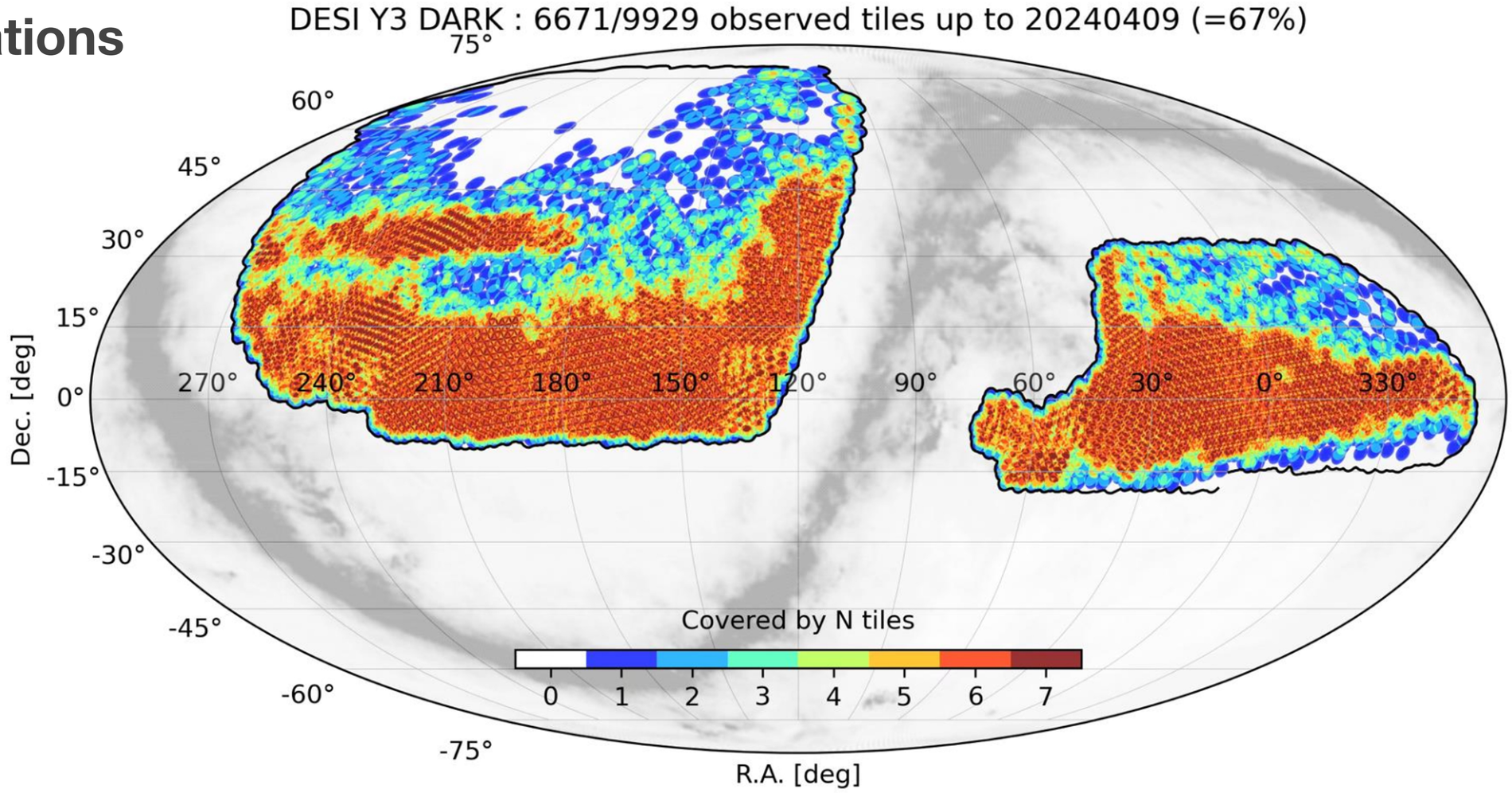

Image credit: DESI

DESI DR3 footprint and coverage

DARK ENERGY SPECTROSCOPIC INSTRUMENT

U.S. Department of Energy Office of Science

First 5 years of observations

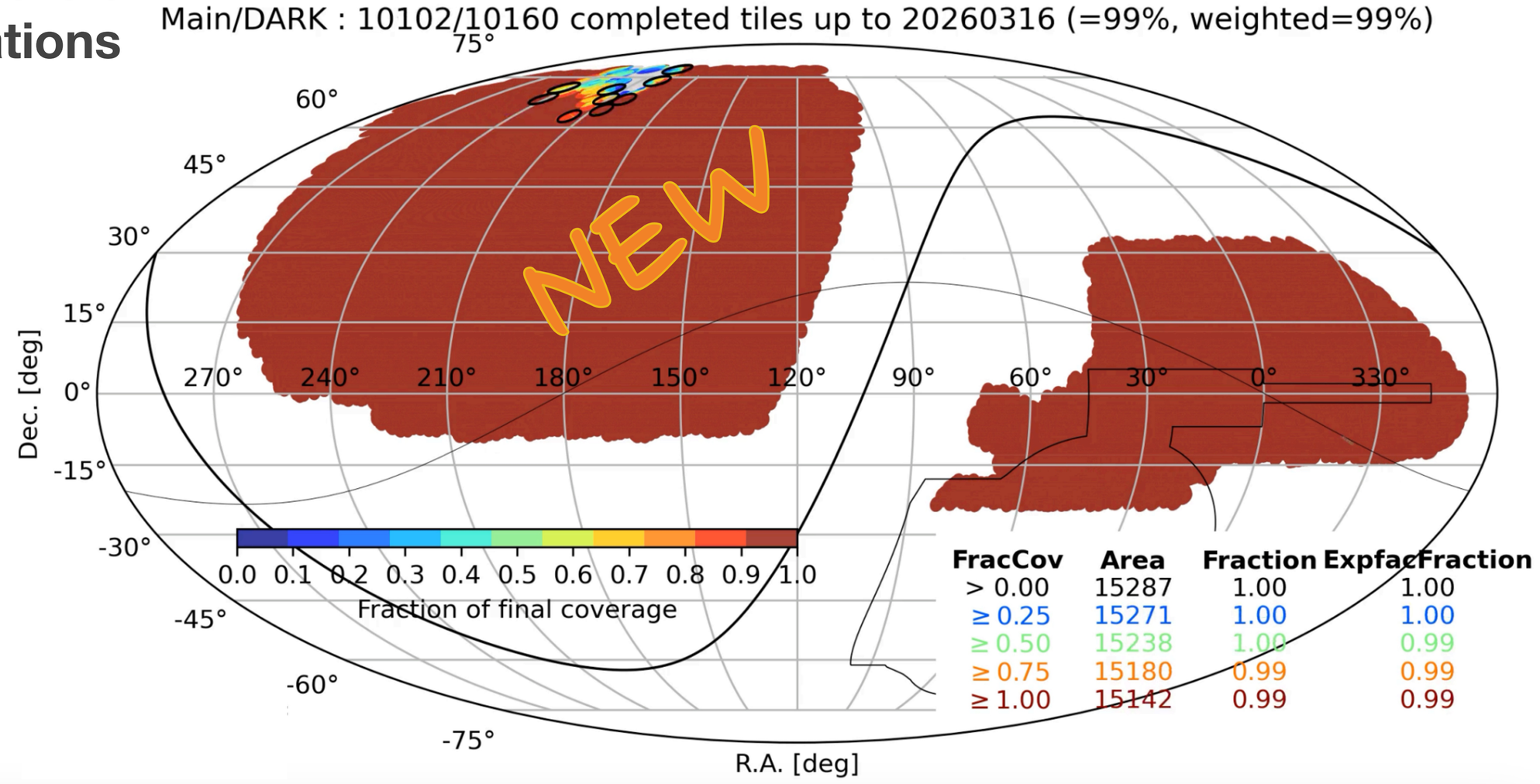

Image credit: DESI

DESI data releases

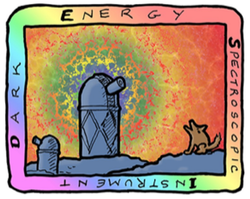

DARK ENERGY SPECTROSCOPIC INSTRUMENT

U.S. Department of Energy Office of Science

- Two data samples currently analysed: DR1 and DR2
- 5.7M redshifts made public in DR1
- 14.3M redshifts in DR2 (currently being analyzed by collaboration)
- Selected from over 30M galaxy and quasar redshifts in 3 years of operation
- Compared to public DR1, **DR2 represents a factor of 2.4 improvement in data volume**

Tracer	DR1	DR2
BGS	300,043	**1,188,526**
LRG	2,138,627	**4,468,483**
ELG	2,432,072	**6,534,844**
QSO	1,223,391	**2,062,839**
Total	6,094,133	**14,254,692**

DESI Data Release 2 (DR2)

DARK ENERGY SPECTROSCOPIC INSTRUMENT

U.S. Department of Energy Office of Science

- DESI DR2 BAO analysis completed! (arxiv/2503.14738 & 14739)
- Remaining DR2 analysis to be finalised this year, including:
  - Galaxy clustering full shape
  - Cross-correlations with weak lensing
  - Cross-correlations with CMB lensing
  - Growth of structure from peculiar velocities
- DR3 BAO expected by 2027

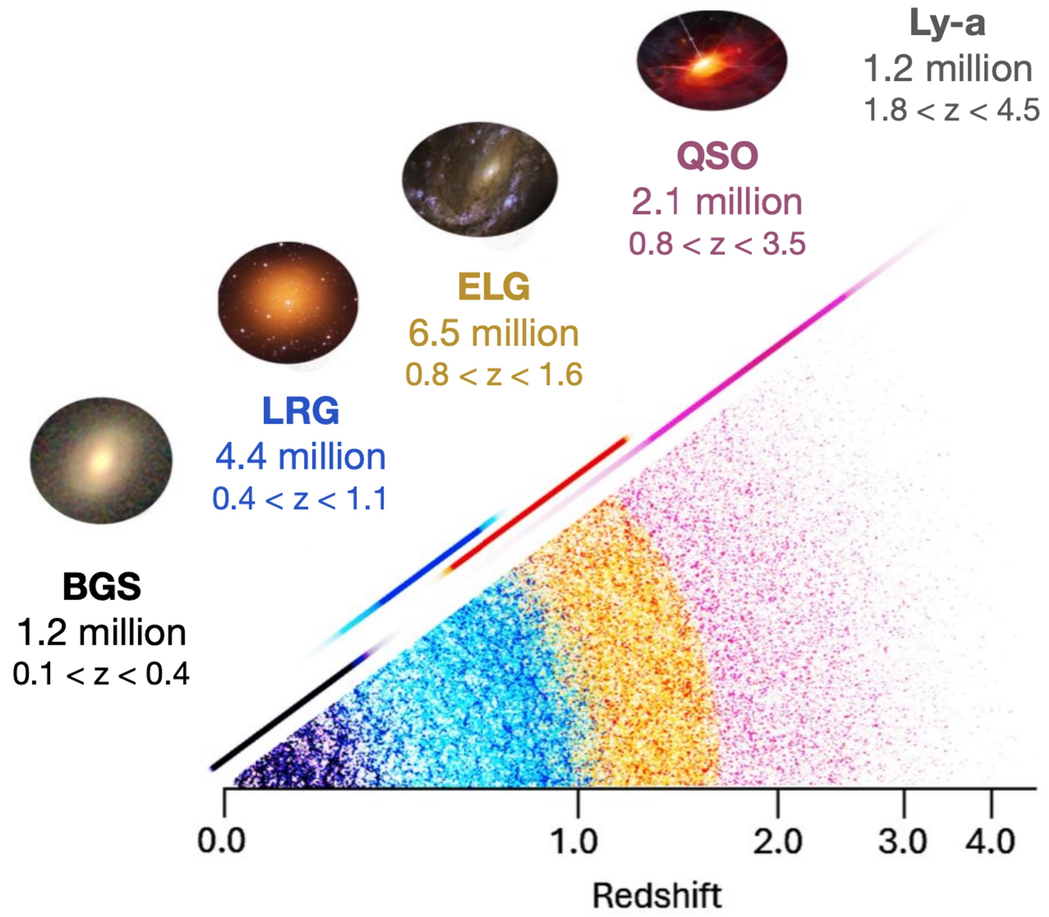

DESI DR2 BAO measurements

DESI DR2 BAO paper: DESI collaboration 2025, arXiv:2503.14738

DARK ENERGY SPECTROSCOPIC INSTRUMENT

U.S. Department of Energy Office of Science

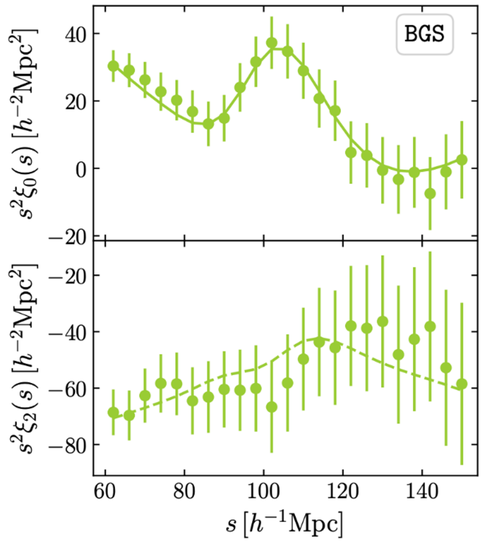

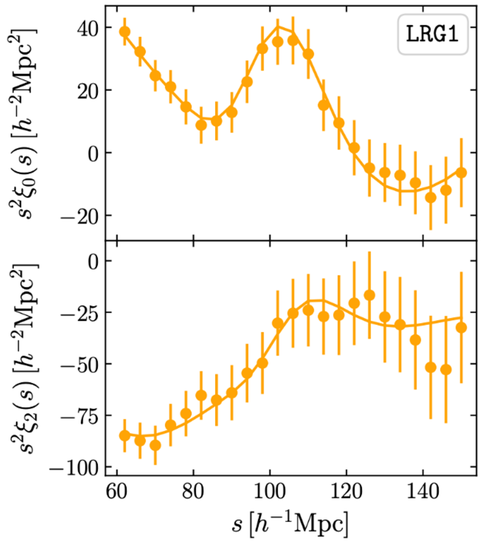

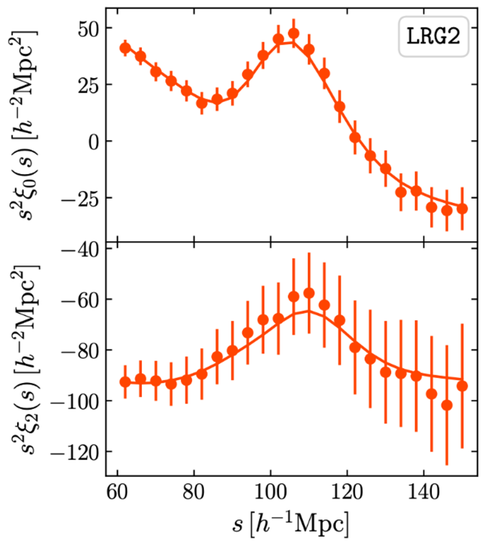

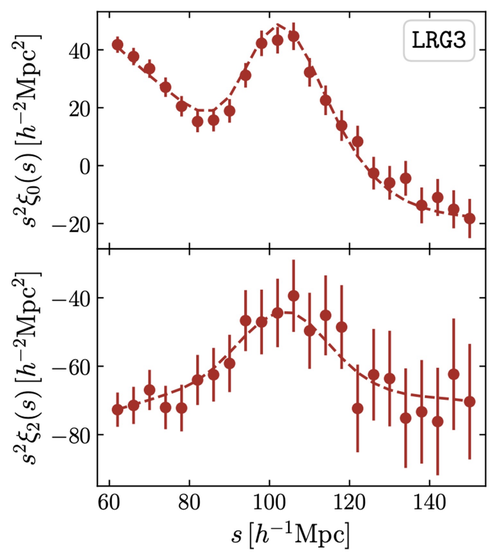

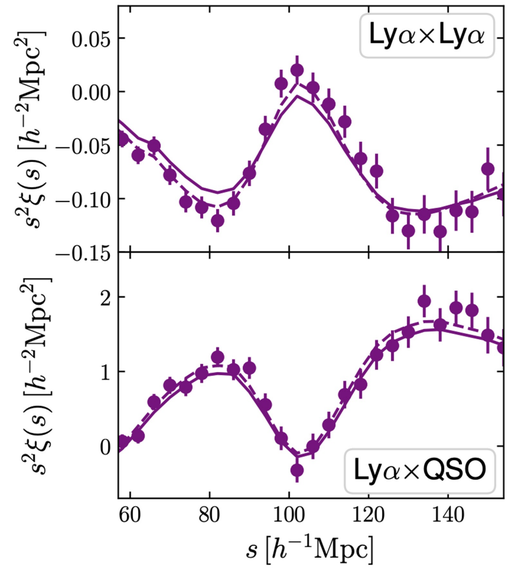

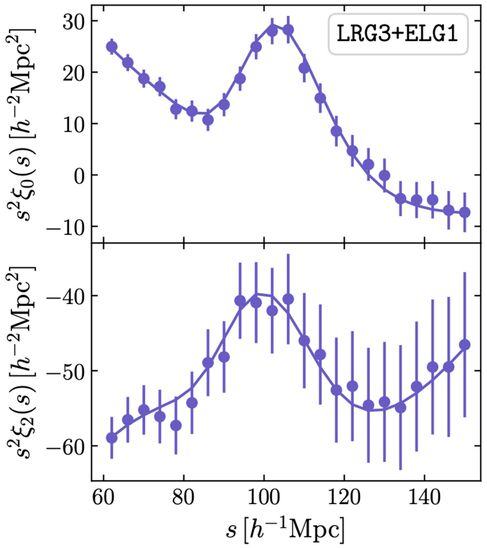

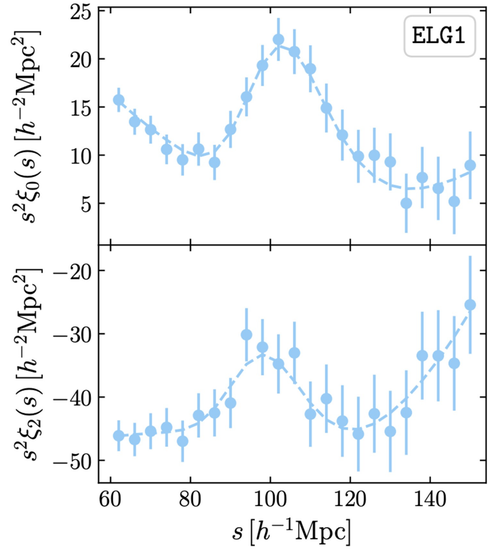

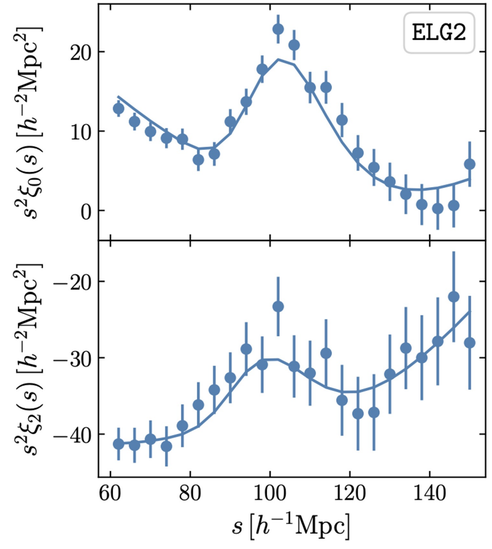

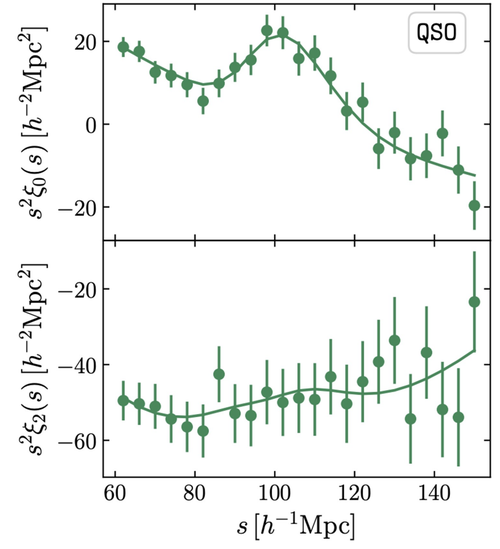

DESI DR2 BAO cosmology

DESI DR2 BAO paper: DESI collaboration 2025, arXiv:2503.14738

DARK ENERGY SPECTROSCOPIC INSTRUMENT
U.S. Department of Energy Office of Science

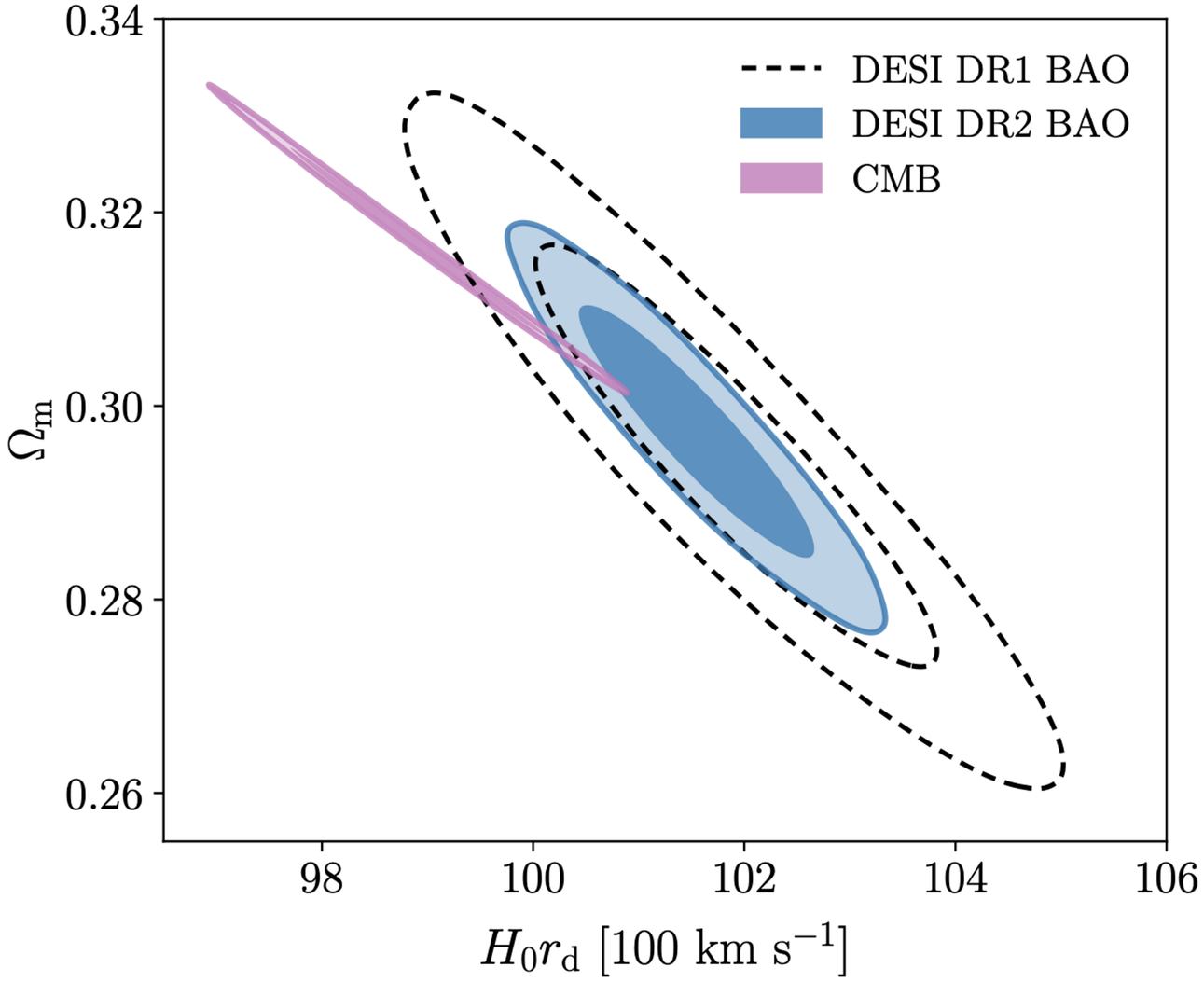

- 40% improvement in the constraints compared to DR1
- Discrepancy between BAO and CMB has increased:

  1.9σ (DR1) → 2.3σ (DR2)

CMB = Planck + ACT lensing


Thank You
annamaria.porredon@ciemat.es